The Canadian Mineralogist
Vol. 52, pp. 809-836 (2014)
DOI: 10.3749/canmin.1400032

PEGMATITIC BERYL AS INDICATOR OF MELT EVOLUTION: EXAMPLE FROM THE VELASCO DISTRICT, PAMPEANA PEGMATITE PROVINCE, ARGENTINA, AND REVIEW OF WORLDWIDE OCCURRENCES

Fernando G. SARDI

Instituto Superior de Correlación Geológica (INSUGEO) - Consejo Nacional de Investigaciones Científicas y Tecnológicas (CONICET), Miguel Lillo 205 (4000), San Miguel de Tucuman, Argentina

Adriana HEIMANN[§]

Department of Geological Sciences, East Carolina University, 101 Graham Building, Greenville, NC 27858, USA

Abstract

Rare-element class, beryl type, beryl-columbite-phosphate subtype pegmatites of the Velasco district from the Pampeana Pegmatite Province, Argentina, contain varieties of green, yellow, and aquamarine beryl. The major and trace element chemistry and dimensions of the unit cell parameters of beryl from ten pegmatites from the Velasco district were used to identify differences among beryl types, determine chromophore elements, and determine the relative degree of fractionation of the pegmatites. Concentrations of Rb, Li, Cs, and Na in all beryls analyzed are among the lowest measured in pegmatitic beryl of similar colors worldwide. Within and among individual pegmatites, an increase in Li and Cs contents and decrease in Na/Li ratios in the order green beryl → yellow beryl → aquamarine suggest that green beryl formed in the early stages of crystallization of the pegmatites while yellow beryl and aquamarine formed from more evolved fluids in the late stages of crystallization. The chemical variations from green beryl to yellow beryl to aquamarine reflect crystallization during melt fractionation and/or crystallization of Fe-Mn phosphate minerals. Beryl from the El Bolsoncito and El Principio pegmatites, with the highest Li and Cs and some of the lowest Fe + Mg contents in the studied beryl, reflects the highest degree of evolution among the Velasco pegmatites. Within individual pegmatites Cr contents in beryl decrease in the order green beryl → yellow beryl, and green beryl → aquamarine, consistent with Cr being a chromophore element for green beryl. Niobium contents increase from green to yellow beryl, and from green beryl to aquamarine, indicating that Nb tends to concentrate in late forms of beryl. The absence of a systematic change in the size of unit cell parameters *a* and *c* with varying compositions and the small size of the *c* parameter reflect the extremely limited incorporation of Li, Na, and Cs in the mineral. A compilation of beryl compositions worldwide shows the highest degree of fractionation for the Tanco, Koktokay No. 3, Minas Gerais, Kaatiala, Namivo, Bikita, Czech Republic, and Greer Lake pegmatites.

Keywords: beryl, granitic pegmatites, mineral chemistry, fractionation, Velasco District, Pampeana Pegmatite Province, Argentina.

Introduction

Beryl is a relatively rare mineral that occurs in a restricted number of geologic settings; among these it is most abundant in granitic pegmatites. It also occurs in hydrothermal deposits associated with granites (*e.g.*, greisen and quartz-cassiterite veins), in rhyolites, and locally in metamorphic rocks (especially emerald-bearing schists, skarns) (*e.g.*, Barton & Young 2002). Beryl appears in nature with different colors as a consequence of elemental substitutions that play a chromatic role in the mineral (*e.g.*, Černý 2002, Přikryl *et al.* 2013). Therefore, the color of beryl can be quite variable: colorless (goshenite), green, translucent green (emerald), yellow (heliodor), light blue (aquamarine), pink (morganite), and white. Because of its rarity, color, large idiomorphic crystals, hardness, and the high degree of translucence and transparency of some crystals, beryl is a valuable and beautiful mineral traded as a precious and semi-precious gemstone and is highly sought for mineral collections. Beryl is also an economically important mineral as one of the main ores of Be used in alloys, wire, nuclear reactors, and on space shuttles (*e.g.*, Barton & Young 2002, Grew 2002).

[§] *Corresponding author e-mail address*: heimanna@ecu.edu

The chemical composition of major and accessory minerals can be utilized to geochemically characterize granitic pegmatites. Among the essential minerals, the most commonly used are feldspars and micas, and their compositions have provided information for typology, mineral exploration, petrogenetic evolution, and degree of magma fractionation (*e.g.*, Černý *et al.* 1985, Morteani *et al.* 1995, Galliski *et al.* 1997, Alfonso *et al.* 2003). Among the accessory minerals used to understand the evolution of pegmatitic fluids is beryl (*e.g.*, Černý & Turnock 1975). In beryl, the concentrations of alkali elements such as Na, Li, and Cs, and of divalent metals like Fe and Mg, have been used to determine the geochemical and paragenetic characteristics of the host pegmatites (*e.g.*, Černý & Turnock 1975, Evensen & London 2002, London and Evensen 2002, Černý 2002, Neiva & Neiva, 2005, Uher *et al.* 2010).

Geochemical studies of beryl in pegmatites from the large and economically important Pampeana Pegmatite Province, Argentina, are very limited. The only available geochemical study of pegmatitic beryl from Argentina is that of beryl in the rare-element class, beryl-columbite subtype pegmatites of the Punillas district, Córdoba (Colombo & Lira 2006). In the Velasco pegmatite district, beryl constitutes the most important economic mineral, and it has been mined, although intermittently, for the last century as a source of beryllium and, most recently, for its gemstones (Saadi 2006, Sardi 2008). However, the chemistry of beryl from this important pegmatite district has yet to be investigated.

This contribution presents a chemical and crystallochemical study of green, yellow, and aquamarine beryl from ten pegmatites from the Velasco district in the Pampeana Pegmatite Province, Argentina. Beryl was characterized geochemically based on major and trace element chemical compositions while X-ray diffraction was used to determine the unit cell parameters. The objectives of this study were to determine: (1) the chemical characteristics of different varieties of beryl; (2) the relationships between beryl composition and color, composition and unit-cell dimensions, and composition and pegmatite melt fractionation; and (3) the relative fractionation of the pegmatites, using the new data and an extensive compilation of chemical compositions of beryl from pegmatites worldwide.

Geologic Setting

Pampeana pegmatite province

The studied pegmatites are located in the Velasco district of the large Pampeana Pegmatite Province (Galliski 1994a, b; Fig. 1a) in the Sierras Pampeanas geologic province in central and northwestern Argentina. The Sierras Pampeanas are underlain by diverse suites of igneous and metamorphic rocks (*e.g.*, Rapela *et al.* 2001a). Pioneer regional studies of the pegmatites in the Province by Herrera (1965, 1968) grouped them into four types based mainly on their internal structure, composition, evolution, and mineralization. Galliski (2009) defined 19 pegmatitic districts within the Province, four of which are muscovite class and located predominantly in the west in terranes of lower metamorphic grade compared to those in the other 15 districts of rare-element class pegmatites. Most of the rare-element class pegmatites belong to the LCT (Li-Cs-Ta) family (classification of Černý 1991 and Černý & Ercit 2005), whereas a small number belong to the NYF (Nb-Y-F) family (Galliski 2009). The Velasco district has been classified as a hybrid LCT–NYF system with rare-element class, beryl type, beryl-columbite-phosphate subtype pegmatites (Galliski 1994a, Galliski 2009, Sardi & Grosse 2005).

Velasco pegmatite district

The Velasco pegmatite district is located in the central and central-eastern section of the Velasco mountain range (Fig. 1b). Regionally, the Velasco mountain range is composed of granitoids of Paleozoic age (Báez *et al.* 2005, Toselli *et al.* 2005) and small outcrops of metapelites and metapsammites that, based on correlation, are designated here as part of the La Cébila formation, which is defined in the Ambato mountain range located nearby to the north (González-Bonorino 1951). Lithologically, the La Cébila formation is composed of phyllites and greywackes with a clastic-marine protolith and experienced low to very low grade regional metamorphism. Paleontological studies of this formation placed the age of sedimentation in the lower Ordovician (Verdecchia *et al.* 2007).

Magmatism in the Velasco range is polyphasic: one episode took place primarily during the middle Ordovician while the other developed during the lower Carboniferous (Toselli *et al.* 2007). The Ordovician granitoids of the NW, W, and central sections of the range are syenogranites and monzogranites with muscovite and biotite, occasionally with cordierite, and they are geochemically peraluminous (Toselli *et al.* 2007). Dating of these granitoids by U-Pb in zircon yielded crystallization ages between 470 and 480 Ma (Pankhurst *et al.* 2000, Rapela *et al.* 2001b, Báez *et al.* 2008). The Ordovician granitoids located to the south have a tonalitic to granodioritic composition with accessory minerals such as allanite, titanite, magnetite, biotite, and hornblende, and are chemically weakly peraluminous to metaluminous (Bellos 2008). The granitoids were affected by upper Silurian – lower Devonian NNW–SSE trending shear zones that formed mylonitic rocks (*e.g.*, Höckenriener *et al.* 2003, López *et al.* 2007).

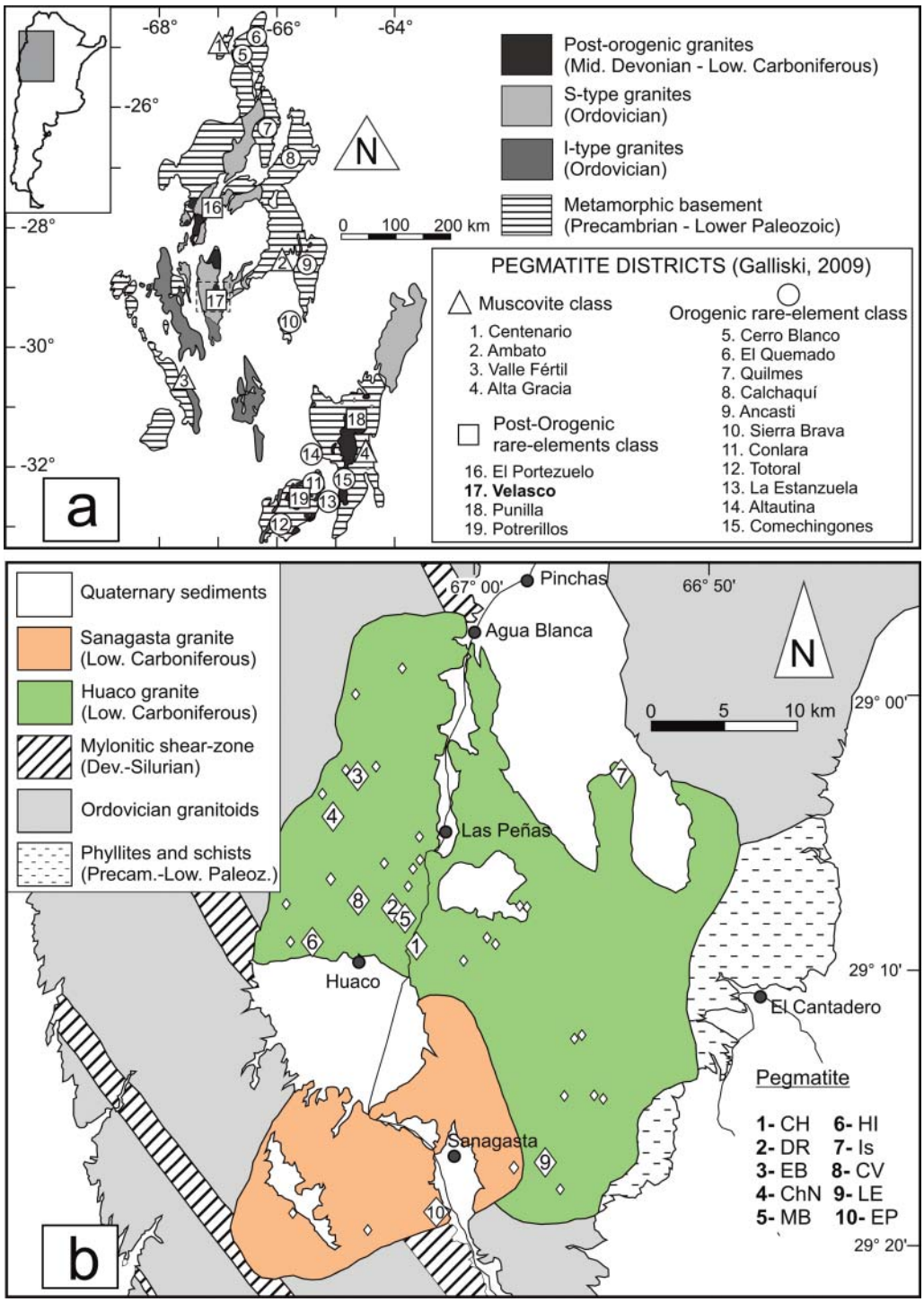

FIG. 1. (a) Simplified geologic map of the Pampeana Pegmatite Province, Argentina, showing the pegmatite districts and the location of the Velasco district. After Galliski (2009). (b) Geologic map of the Velasco district showing the location of the studied pegmatites. Modified after Sardi *et al.* (2010). Abbreviations of pegmatite names according to Table 1.

The Carboniferous granitoids of the Velasco range are located in the far north and northwest sections and in the central and central-western parts of the range. The granitoids are post-tectonic, not affected by deformation, and have a syenogranitic and monzogranitic composition with biotite and muscovite as main accessory minerals. They have been dated by U-Pb between 334 and 353 Ma (Báez *et al.* 2004, Dahlquist *et al.* 2006, Grosse *et al.* 2009). The parental granitoids of the beryl-bearing pegmatites from the Velasco district belong to this group of granitoids and correspond to the Huaco (Toselli *et al.* 2000) and Sanagasta granitoids (Grosse & Sardi 2005) (Fig. 1b). The Huaco granitoid is white, porphyritic, and is characterized by microcline megacrysts, whereas the Sanagasta granitoid is also porphyritic, but pink, and is characterized by incipient replacement of microcline by plagioclase. The contact between both granitoid bodies is transitional and the compositions are similar for both and correspond to monzogranite and syenogranite with accessory biotite, muscovite, apatite, zircon, and ilmenite (Grosse *et al.* 2009). Chemically, the granitoids are peraluminous, rich in SiO_2 and alkalis, especially K_2O, and formed from a predominantly crustal source (primarily derived from the Ordovician granitoids) and a minor mantle component (Grosse *et al.* 2009). It is worth noting that in a more recent geological, petrographic, and geochemical study the Huaco and Sanagasta granitoids were classified as A-type granites (Dahlquist *et al.* 2010).

Characteristics of the pegmatites

In Table 1 we present the type of beryl, coexisting minerals, and the geographic coordinates of the 10 pegmatites selected for this study, whereas Figure 1b shows their areal distribution. Geometrically, the pegmatites have ellipsoidal/oval shapes or semi-circular shapes, some are elongated, and others are discontinuous. The dimensions of the pegmatitic bodies are relatively small, with the longer axes not surpassing 200 m (Sardi 2005). The Cuesta de Huaco pegmatite is a small lenticular dike with a maximum thickness of 40 cm and maximum length of 10 cm.

In general, the pegmatites, with the exception of Cuesta de Huaco, have simple zoning consisting of a border zone ranging from a few centimeters to a few decimeters in thickness, an intermediate zone up to several tens of meters wide, and a quartz core that can be up to a few meters wide or sometimes absent. The border zone is a felsic, aplitic (or, in places, a medium grained equigranular, granitic) rock with granodioritic or monzogranitic composition, rich in quartz, and equal proportion of plagioclase and microcline (Sardi *et al.* 2010). The intermediate zone is composed of quartz and feldspar (potassic and plagioclase) as essential minerals, and muscovite (very rarely biotite), beryl, phosphates (mainly fluorapatite and triplite), and tourmaline as main accessory minerals. It is worth noting that in an unpublished report (Ricci 1971) and a more recent summary of the pegmatites (Cravero 2005) the occurrence of accessory spodumene in the intermediate zone was mentioned for the pegmatites Huaco I, Cora Vivi, and La Esperanza.

Sampling and Analytical Methods

Representative samples of beryl derived from the intermediate zone of the pegmatites were selected for study (Table 1). Sampling was performed preferentially in the dumps because this is where the best specimens were found. In many instances each sample contained beryl of different colors, in which case manual selection was done to separate specimens by color. Thus, for some pegmatites we obtained two or three of the varieties of beryl studied here. Compositional zoning in the beryl samples studied is minimal and heterogeneous, which justifies crushing complete crystals. Following a first coarse crushing of the sample, the beryl was purified by extracting impurities of quartz, feldspar, and muscovite using a binocular lens, fine tweezers, and needles. Finally, each sample of pure beryl was ground to a fine powder using a carbon tungsten ring mill in the Laboratory of Petrology of the Instituto Superior de Correlación Geológica (INSUGEO; Tucumán, Argentina) and a carbon tungsten ball mill in the Department of Geological Sciences, East Carolina University (ECU). The powder generated was used to obtain major and trace element bulk beryl chemical compositions and to perform X-ray diffraction (XRD) analysis to determine the values of unit-cell parameters and to check the purity of the powdered beryl samples.

Twenty five samples of finely powdered beryl were chemically analyzed. Eleven of these powdered beryl samples were analyzed commercially at Actlabs (Canada) for major, minor, and trace elements after total fusion with lithium metaborate/tetraborate (except for Be). The resulting molten bead was rapidly digested in a weak nitric acid solution to assure that the entire sample, including SiO_2, rare earth elements (REEs), and other high-field-strength elements, was dissolved. Major and trace elements were analyzed by inductively coupled plasma-mass spectrometry (ICP-MS). The remaining 14 powdered beryl samples were analyzed for major and some trace elements (except Li and Be) by X-ray fluorescence (XRF) (after total fusion by lithium metaborate) and for REEs by ICP-MS at the Instituto Geológico y Minero de España (IGME). Determinations of Li and Be were made after acid digestion ($HF + HClO_4 + HNO_3$, followed by drying and final dissolution in HCl 10%) by atomic absorption spectrophotometry (AAS) with a Varian SpectrAA FSS 220 instrument, and ICP atomic emission spectrometry (AES) with a

TABLE 1. SUMMARY OF THE MAIN CHARACTERISTICS OF PEGMATITIC BERYL, ASSOCIATED MINERALS, HOST PEGMATITE NAME, AND SYMBOLS USED IN FIGURES, VELASCO DISTRICT, ARGENTINA

Pegmatite	Nomenclature	Symbol	Beryl Type and Associated Minerals	Coordinates
Chivo Negro	ChN	△	Light **green** dominant; **yellow** and **aquamarine** less abundant. Associated with feldspars, quartz, and muscovite	29° 04' 22" S 67° 06' 08" W
Cora Vivi	CV	◆	**Yellow** and **green** associated most commonly with quartz. Aquamarine minor	29° 07' 25" S 67° 05' 01" W
Cuesta de Huaco	CH	✚	**Yellow**, rarely green; commonly associated with quartz	29° 08' 34" S 67° 02' 25" W
Diadema Riojana	DR7, DR8, DR8-he	□	**Yellow**, **heliodor**, and in places light green. Associated with quartz and muscovite	29° 07' 46'' S 67° 03' 22'' W
El Bolsoncito	EB	◊	Light **green** dominant. **Aquamarine** less abundant. Associated with feldspars, quartz, and muscovite	29° 02' 54" S 67° 05' 09" W
El Principio	EP	●	**Aquamarine**, most commonly associated with quartz and in less degree feldspars	29° 19' 29" S 67° 01' 14" W
Huaco I	HI	*	**Yellow**, **green**, and **aquamarine**. Associated with feldspars and quartz, less common with muscovite	29° 09' 17" S 67° 06' 52" W
Ismiango	Is	○	**Yellow** dominant. Associated with muscovite, quartz, and feldspars	29° 02' 42" S 66° 51' 15" W
La Esperanza	LE	▲	**Yellow** and **green** associated with muscovite and K-feldspar. Less common aquamarine associated with quartz	29° 17' 23'' S 66° 57' 18'' W
Mogote Blanco	MB	X	Green and **yellow** dominant; **aquamarine** subordinated. Associated with muscovite and feldspars	29° 07' 56" S 67° 03' 06" W

Note: In bold is the type of beryl analyzed in each pegmatite in this study.

Varian Vista-MPX instrument), respectively, in the same laboratory.

A PANalytical X'Pert PRO X-ray diffractometer housed in the Department of Geological Sciences at ECU was utilized for XRD analysis of 25 crystals. The following working conditions were used: Cu*K*α radiation, five scans for each mineral, step size of 0.017º (2θ), and step time of 10 seconds, and a 2θ of 25º–65º. Processing of XRD patterns was done using the X'Pert HighScore software by PANalytical.

Ten polished thin sections containing representative beryl crystals were prepared (Vancouver Petrographics, Canada) for electron microprobe (EMP) analysis of major and minor elements, which was conducted using a JEOL JXA-8530 Hyperprobe housed at Fayetteville State University (NC). Analytical conditions were an accelerating voltage of 15 kV, a probe current of 10 nA, and counting times for peaks and background of 10 s and 5 s, respectively. Natural and synthetic standards were used, including albite (Na), almandine (Si, Al, Fe, Mg), bustamite (Ca, Mn), and sanidine (K). Beryllium oxide contents were calculated by stoichiometry using the Al_2O_3 and SiO_2 contents and assuming ideal beryl ($Be_3Al_2Si_6O_{18}$). Transects across crystals from rim to rim passing through the center, as well as individual spot analyses, were performed with a total of 344 individual analyses obtained from 50 beryl crystals.

Results

Occurrence of beryl

Beryl occurs almost exclusively in the intermediate zone of the pegmatites where it is found as isolated crystals or in groups with a maximum modal abundance of 7%. Beryl is always spatially associated with anhedral grey quartz, feldspars, and masses of muscovite (Fig. 2). Beryl of different colors was observed included in all three minerals and no relationship was found between the color of beryl and the type of associated minerals. In these pegmatites beryl is idiomorphic with well-developed hexagonal prisms of variable size (Fig. 2). The most common forms are first-order prisms and basal pinacoids. Some crystals

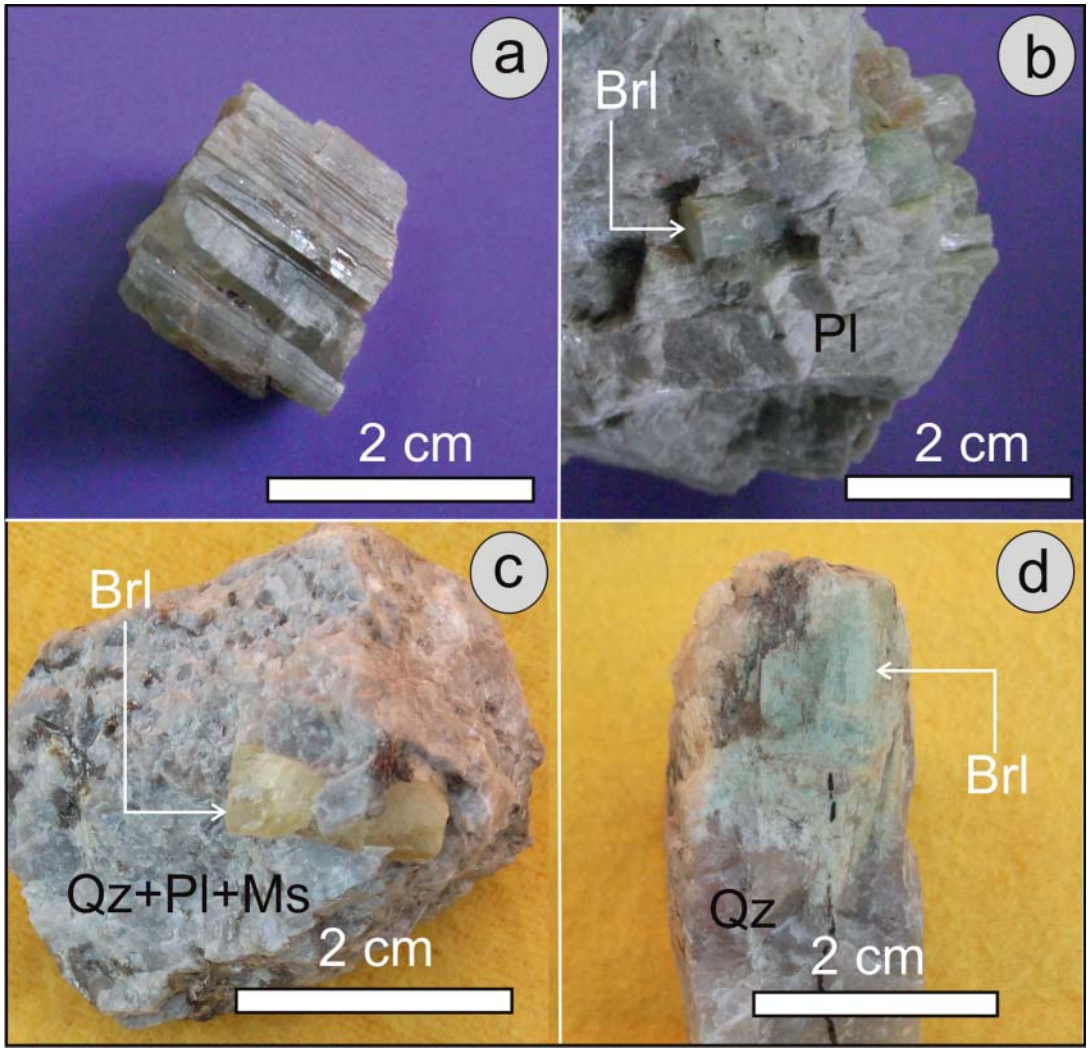

FIG. 2. Examples of beryl in pegmatites from the Velasco district. (a) Light green beryl showing striations along the length of the crystal. Cora Vivi (CV) pegmatite. (b) Idiomorphic crystal of green beryl (Brl) in plagioclase (Pl) matrix. El Bolsoncito (EB) pegmatite. (c) Idiomorphic crystal of yellow beryl in a quartz (Qz)-plagioclase-muscovite (Ms) matrix. Cora Vivi pegmatite. (d) Aquamarine in a quartz matrix. La Esperanza (LE) pegmatite.

are wedge-shaped and narrower at one end. The basal sections of the largest crystals reach 6 cm in diameter and the visible length of the longest crystals is up to 12 cm (Sardi 2008). Where beryl is associated with muscovite it is very thin and long, whereas where it coexists with greyish quartz its hexagonal basal section is larger and the crystal longer. In general, prisms of green beryl have larger dimensions in basal sections and are shorter than prisms of yellow beryl. The {0001} cleavage is generally not well developed but can be visible. The dominant colors of beryl from the Velasco district are green and yellow in light and dark tones. Less common is the aquamarine variety with light blue and turquoise tones, and rarer is heliodor (gem-quality transparent yellow). In some pegmatites beryl is present in one color while in others it occurs in all varieties (Table 1).

Major and minor element chemical composition of beryl

Representative major and minor element chemical compositions of beryl obtained from bulk powders (by XRF, ICP-MS, AAS, ICP-AES) and individual

crystals (EMP analysis) are presented in Tables 2 and 3, respectively, while the entire data set can be found in Electronic Appendix Table A1. Iron contents do not exceed 1.6 wt.% FeO (Fig. 3a). Green beryl has slightly higher average concentration of Fe (0.57 wt.% FeO) compared to yellow beryl (0.46 wt.% FeO) and aquamarine (0.48 wt.% FeO) (EMP compositions; Fig. 3a). In bulk beryl, the average iron contents for yellow and green beryl are similar. Yellow and green beryl have similar Mn ranges, whereas aquamarine has lower Mn contents (avg. 0.04 wt.% MnO; Fig. 3b). Aquamarine contains slightly higher average Mg contents (0.048 wt.% MgO) than green beryl (0.03 wt.% MgO) and yellow beryl (0.018 wt.% MgO) when measured *in situ* (EMP; Table 3; Fig. 3c), even though they are all very low and similar. Alkali element contents are low, with yellow beryl having the highest concentration of Na (up to 0.45 wt.% Na_2O) and K (up to 0.22 wt.% K_2O) (bulk beryl; Table 2; Fig. 3d, e). Water contents were calculated using the expression originally recommended by Giuliani *et al.* (1997) and later modified (Giuliani *pers. comm.* with Groat *et al.* 2010), H_2O wt.% = (0.84958 × Na_2O wt.%) + 0.83731, which yielded a range from 0.99 to 1.22 wt.% H_2O for all beryl varieties analyzed.

Finally, elemental profiles of hexagonal basal sections (pinacoid face [0001]) of green and yellow beryl based on rim–center–rim EMP transects show a variable but random compositional zonation in Na and Fe + Mg + Mn. For example, from the center to the rim some crystals show an increase in Na_2O and a decrease in (FeO + MgO + MnO), while others show the opposite. However, due to the very low contents of these elements in beryl, the observed variations of only up to 0.2 wt.% in the oxides of these elements are likely within analytical error for EMP and insignificant, and will not be discussed further.

Trace element chemical composition of beryl

Representative trace element contents, including rare earth elements (REEs), of beryl are presented in Table 2, while the entire data set is included in Electronic Appendix Tables A1–A3 (available from the MAC Depository of Unpublished Data, document pegmatitic beryl CM52_10.3749/canmin.1400032). A comparative multi-element spider diagram of beryl was constructed plotting the average of trace element contents for green and yellow beryl normalized to the average aquamarine composition to identify differences among the three types of beryl (Fig. 4a). Comparatively, yellow beryl has greater average contents of Ba (7.3 ppm), Sr (3.0 ppm), Zn (183 ppm), Ga (26.5 ppm), Rb (35.1 ppm), Nb (11.5 ppm), Cs (535 ppm), and REEs (2.8 ppm), and lower average contents of Sc (2.7 ppm) than aquamarine and green beryl. Yellow and green varieties of beryl have similar average Ge (~1.4 ppm) contents and are depleted in this element compared to aquamarine (3.9 ppm Ge). A relative enrichment in Cr (avg. 51.2 ppm), Tl (avg. 0.65 ppm), and Sc (avg. 5.3 ppm), and depletion in Li (avg. 22.2 ppm), Co (avg. 109 ppm), Cs (avg. 327 ppm), and Ta (avg. 10.5 ppm) is observed in green beryl compared to the other beryl varieties. Aquamarine has higher average contents of Li (66.4 ppm), Y (11 ppm), and Ge (3.9 ppm) compared to yellow and green beryl. Overall, the Ta and Nb contents are low, reaching ~26 ppm Nb in yellow beryl and ~31.6 ppm Ta in green beryl and aquamarine (Figs. 3m, n; 4). The average concentration of Nb in yellow beryl is higher than in the other two types, which have similar average contents (Figs. 3m; 4a). The ranges of Ta contents in green beryl and aquamarine are similar but the averages are similar for yellow beryl and aquamarine (Fig. 3n).

The REE contents of beryl are always below the chondrite, with total values below 6 ppm (Fig. 4b; Tables 2, A3). Chondrite-normalized REE patterns have slightly decreasing LREE profiles from La to Eu, slightly increasing HREE shapes, strong negative Eu anomalies, and overall flat-trending profiles. An exception is a green beryl, which has increasing HREE contents from Gd to Lu and higher HREEs than the other varieties of beryl. Aquamarine has the lowest REE contents and for most samples HREEs are below detection limits (Fig. 4b).

Unit cell parameters

Unit-cell parameters were measured for 25 beryl crystals from the Velasco district pegmatites (Table 4; Electronic Appendix Fig. A1). Several separate crystals were analyzed for some samples, whereas for smaller samples of beryl more than one small crystal combined were analyzed. We note here that not all the crystals studied with XRD were analyzed chemically.

The sizes of the unit-cell parameters fall within those measured previously for other pegmatitic beryl worldwide. The absolute values and average of the unit cell parameter *a* and the *c/a* ratio are similar for the three varieties of beryl (*a* = 9.201–9.217 Å; avg. *a* = 9.211 Å; *c/a* = 0.997–1.002; Table 4). However, yellow varieties of beryl have the highest values of the *a* parameter, aquamarine the highest *c* value, while the lowest *c* values were measured from green beryl (Fig. A1). No correlation was found between the size of the unit-cell parameters *a* and *c* and the amounts of Li (Fig. A1a), Fe + Mg (Fig. A1b), and alkalis (Na + K + Rb + Cs) in beryl (Fig. A1c).

Discussion

In this section we first make some crystallochemical considerations about beryl from the Velasco district that, along with their chemical compositions, are used to infer the degree of fractionation of the

TABLE 2. REPRESENTATIVE MAJOR, TRACE, AND RARE EARTH ELEMENT CONTENTS OF BERYL IN PEGMATITES, VELASCO DISTRICT

	Green Beryl (G)			Yellow Beryl (Y)			Aquamarine (Aq)		
Sample	EB-G	EB*'-G	ChN*-G	DR8*-Y	HI-Y	MB*-Y	EP*-Aq	HI-Aq	MB-Aq
SiO_2 (wt.%)	65.76	65.29	64.94	64.47	63.59	64.81	65.23	64.3	64.95
Al_2O_3	18.90	18.49	18.20	18.11	17.76	18.30	18.42	18.86	18.42
FeO^t	0.91	0.66	0.72	0.59	1.62	0.57	0.57	0.69	1.24
MnO	0.011	0.005	0.385	0.107	0.027	0.018	0.004	0.014	0.011
MgO	0.03	–	–	0.02	0.02	–	–	–	0.03
CaO	0.03	–	–	0.05	0.03	0.17	–	0.02	0.02
BeO	13.81	12.91	11.91	12.74	14.07	12.00	12.21	12.76	12.64
Na_2O	0.38	0.26	0.27	0.29	0.45	0.20	0.22	0.33	0.34
K_2O	0.07	–	–	0.05	0.13	0.02	–	0.07	0.08
LOI	1.62	1.44	1.46	1.71	1.75	1.56	1.43	1.76	1.83
Total	101.52	99.06	97.89	98.14	99.45	97.65	98.08	98.80	99.56
Sc (ppm)	2.0	1.4	8.3	–	2.0	3.0	–	–	5.0
Li	—	27.1	19.0	40.6	—	31.1	60.6	—	—
V	6.0	3.0	–	6.0	7.0	2.0	2.4	–	–
Ba	–	–	5.3	4.0	–	1.0	–	3.0	
Sr	–	–	1.2	–	–	1.0	–	–	–
Y	–	–	3.3	2.0	–	4.0	–	–	–
Cr	–	45.0	50.1	–	–	7.0	33.0	–	–
Co	65	78	68	53	266	217	154	119	196
Zn	180	132	184	290	160	70	145	340	130
Ga	20	22	23	25	31	–	19	23	26
Ge	–	2.0	1.4	1.0	1.0	–	18.5	1.0	1.0
Rb	26	23	25	41	33	22	34	20	23
Nb	2.0	2.3	4.4	7.0	10.0	8.0	3.7	2.0	3.0
Cs	370	519	167	577	535	—	730	478	207
Ta	4.8	4.7	3.9	10.3	16.8	–	31.6	6.2	12.0
Tl	0.1	0.4	0.4	0.2	0.2	–	0.4	0.1	–
Th	0.1	–	1.5	1.0	6.0	–	12.6	0.1	0.2
La	0.2	0.1	0.6	0.1	0.6	—	0.1	0.4	0.3
Ce	0.3	0.2	1.3	0.5	0.9	—	0.2	0.3	0.5
Pr	–	0.02	0.16		0.15	—	0.02	0.05	0.06
Nd	0.2	0.03	0.5	0.2	0.5	—	0.02	0.2	0.3
Sm	–	0.02	0.2	0.1	0.2	—	0.02	–	–
Eu	–	–	0.03	–	–	—	–	–	–
Gd	–	0.02	0.2	0.2	0.2	—	0.02	–	–
Tb	–	0.01	0.05	–	–	—	–	–	–
Dy	0.1	0.1	0.3	0.5	0.3	—	0.02	–	–
Ho	–	0.01	0.06	–	–	—	–	–	–
Er	–	0.04	0.18	0.30	0.20	—	0.01	–	–
Tm	–	0.01	0.03	–	0.06	—		–	–
Yb	–	0.06	0.23	0.50	0.60	—	0.02	–	–
Lu	–	0.01	0.03	0.09	0.13	—	–	–	–

Bulk beryl analyses by ICP-MS, ICP-AES (Be), and AAS (Li); ' Additional sample, – Not detected, — Not determined, * Analysis at IGME (Spain), rest in ActLabs (Canada). The different number of significant figures for some REEs is due to analyses obtained from different laboratories.

individual pegmatites. We follow this with a discussion of the relationships between color, composition, and size of unit-cell parameters, chromophore elements, and the relative degree of evolution of beryl varieties within a given pegmatite. Finally, the data obtained here combined with an extensive review of previously published compositions of pegmatitic beryl worldwide are used to make observations about the

TABLE 3. REPRESENTATIVE MAJOR AND MINOR ELEMENT COMPOSITIONS OF BERYL IN PEGMATITES, VELASCO DISTRICT

wt.%	CH-Y *n*=5	Is-Y *n*=4	DR8-Y *n*=4	EB-G *n*=4	EB-G *n*=4	EB-G *n*=1	ChN-Aq *n*=5	ChN-Aq *n*=3	ChN-Aq *n*=5
SiO_2	66.25	65.44	65.78	66.73	67.02	67.08	66.79	66.59	65.97
Al_2O_3	18.07	17.76	17.44	17.34	17.81	17.71	17.61	17.91	17.93
FeO	0.380	0.451	0.407	0.637	0.573	0.702	0.476	0.482	0.478
MgO	0.030	0.012	0.022	0.023	0.039	0.035	0.048	0.007	0.049
MnO	0.038	0.042	0.039	0.068	0.071	0.099	0.036	0.050	0.041
BeO*	13.68	13.50	13.50	13.64	13.76	13.76	13.69	13.71	13.61
CaO	0.02	0.02	0.05	0.02	0.01	—	0.02	0.01	0.01
Na_2O	0.08	0.12	0.24	0.12	0.17	0.15	0.15	0.17	0.16
K_2O	0.01	0.01	0.01	0.01	0.04	0.02	0.02	0.01	0.02
Total	98.55	97.36	97.49	98.58	99.50	99.56	98.84	98.94	98.27
apfu based on 18 oxygen atoms									
Si (*T*1)	6.029	6.033	6.057	6.078	6.051	6.056	6.064	6.042	6.028
Be (*T*2)	2.990	2.988	2.985	2.983	2.984	2.982	2.985	2.987	2.987
Al	1.938	1.929	1.891	1.860	1.895	1.884	1.883	1.915	1.930
Fe	0.029	0.035	0.031	0.048	0.043	0.053	0.036	0.037	0.037
Mn	0.003	0.003	0.003	0.005	0.005	0.008	0.003	0.004	0.003
Mg	0.004	0.002	0.003	0.003	0.005	0.005	0.006	0.001	0.007
Σ*O*	1.974	1.969	1.929	1.917	1.949	1.949	1.929	1.956	1.977
Ca	0.001	0.002	0.005	0.001	0.001	—	0.001	0.001	0.001
Na	0.013	0.022	0.043	0.021	0.029	0.026	0.027	0.029	0.029
K	0.001	0.001	0.001	0.002	0.004	0.002	0.002	0.001	0.002
Σ*Ch*	0.016	0.025	0.049	0.024	0.034	0.028	0.030	0.031	0.031

Obtained by EMPA. — Not detected, * Calculated by stoichiometry assuming an ideal beryl formula. See text for details.

relationships between beryl's color, composition, and pegmatite melt evolution.

Crystallochemistry

The structure of beryl was determined by Bragg & West (1926) and later refined by Gibbs *et al.* (1968) and consists of layers of rings with 6 Si–O tetrahedra (*T*1), which are linked vertically and laterally by Be–O tetrahedra (*T*2) and Al–O octahedra (*O*). The centers of the Si rings contain channels (*Ch*) that tend to be occupied by large components (Černý 2002) such as alkali elements and water. The '2a' position in the channels between the 6 ring of Si tetrahedra is preferentially occupied by alkalis (Na, Cs, Rb, in order of importance; Aurisicchio *et al.* 1988), whereas the '2b' position in the center of each ring is mainly occupied by water molecules (Hawthorne & Černý 1977) and to a minor degree by hydroxyl ions and F. Isotani *et al.* (1989) reported the presence of Fe^{2+} in the channels. The octahedral sites that Al^{3+} preferentially occupies can accommodate Sc, Cr, Mg, Mn, and possibly Ca instead of Al, and charge balance is achieved by incorporation of alkalis in the channels (*e.g.*, Hawthorne & Černý 1977, Sherriff *et al.* 1991, Černý 2002, Aurisicchio *et al.* 2012).

Based on the chemical compositions obtained for bulk beryl (Table A1), the formulas for each of the studied beryl types from the Velasco district, using average values of the most important components, are:

Green beryl:

$^{Ch}(Na_{0.047}, K_{0.002}, Cs_{0.001})^{T2}(Be_{2.809}, Li_{0.002})_{2.811}{}^{O}(Al_{2.006}, Fe_{0.056}, Mn_{0.006}, Mg_{0.001})_{2.069}{}^{T1}Si_{6.031}O_{18}$

Yellow beryl:

$^{Ch}(Na_{0.053}, K_{0.009}, Cs_{0.002})^{T2}(Be_{2.883}, Li_{0.003})_{2.886}{}^{O}(Al_{2.000}, Fe_{0.072}, Mn_{0.009}, Mg_{0.004})_{2.085}{}^{T1}Si_{5.977}\ O_{18}$

Aquamarine:

$^{Ch}(Na_{0.053}, K_{0.005}, Cs_{0.002})^{T2}(Be_{2.793}, Li_{0.005})_{2.798}{}^{O}(Al_{2.014}, Fe_{0.064}, Mg_{0.003}, Mn_{0.001})_{2.082}{}^{T1}Si_{6.024}\ O_{18}$

where *Ch* is the 'channel', *T*2 and *T*1 are the tetrahedral sites for Be and Si, respectively, and *O* is the octahedral site.

Beryl from the Velasco district shows a very weak positive to absent correlation between Be and Li (Fig. A2a), indicating a very minor to absent substitution of Li at the tetrahedral position (*T*2). A weak negative correlation between Fe+Mg and Al evidences a small substitution of Fe+Mg at the octahedral position (Fig. 5; A2b). Aluminum at the octahedral position is also substituted by trace Mn and Cr. The charge deficit that is introduced by these substitutions is

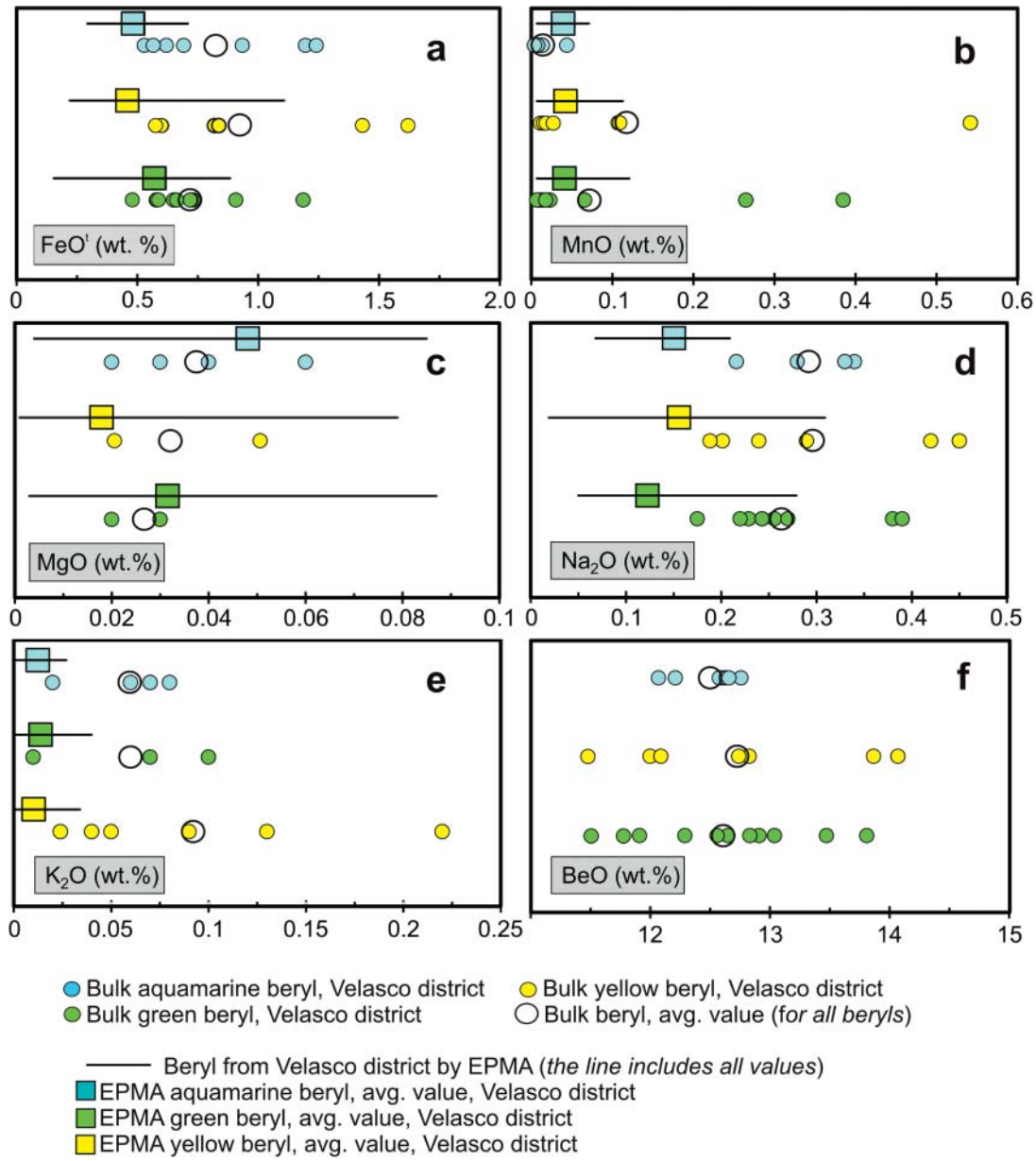

FIG. 3. Diagrams showing the major, minor, and trace element contents of beryl from the Velasco district. (a) FeO^t (wt.%) from EMP analysis and recalculated from bulk beryl analyses. (b) MnO (wt.%). (c) MgO (wt.%). (d) Na_2O (wt.%). (e) K_2O (wt.%). (f) BeO (wt.%). (g) Li (ppm). (h) Na/Li (based on ppm). (i) Rb (ppm). (j) Cs (ppm). (k) V (ppm). (l) Cr (ppm). (m) Nb (ppm). (n) Ta (ppm).

compensated by the incorporation of large monovalent alkaline ions (Na dominantly, up to 0.45 wt.% Na_2O, and Cs) in the channels. The substitutions for the octahedral (*O*) position can be expressed by $^{O}Al = {}^{O}R^{+3} + {}^{Ch}\square$ and $^{O}Al = {}^{O}R^{+2} + {}^{Ch}A^{+1}$, and for the tetrahedral (*T*2) site the substitution is $^{T2}Li + {}^{Ch}A^{+1} = {}^{T2}Be + {}^{Ch}\square$, where in our case R^{+3} represents Fe^{3+} and/or Cr, R^{+2} represents mostly Fe^{2+}, A^{+1} represents Na^{+},

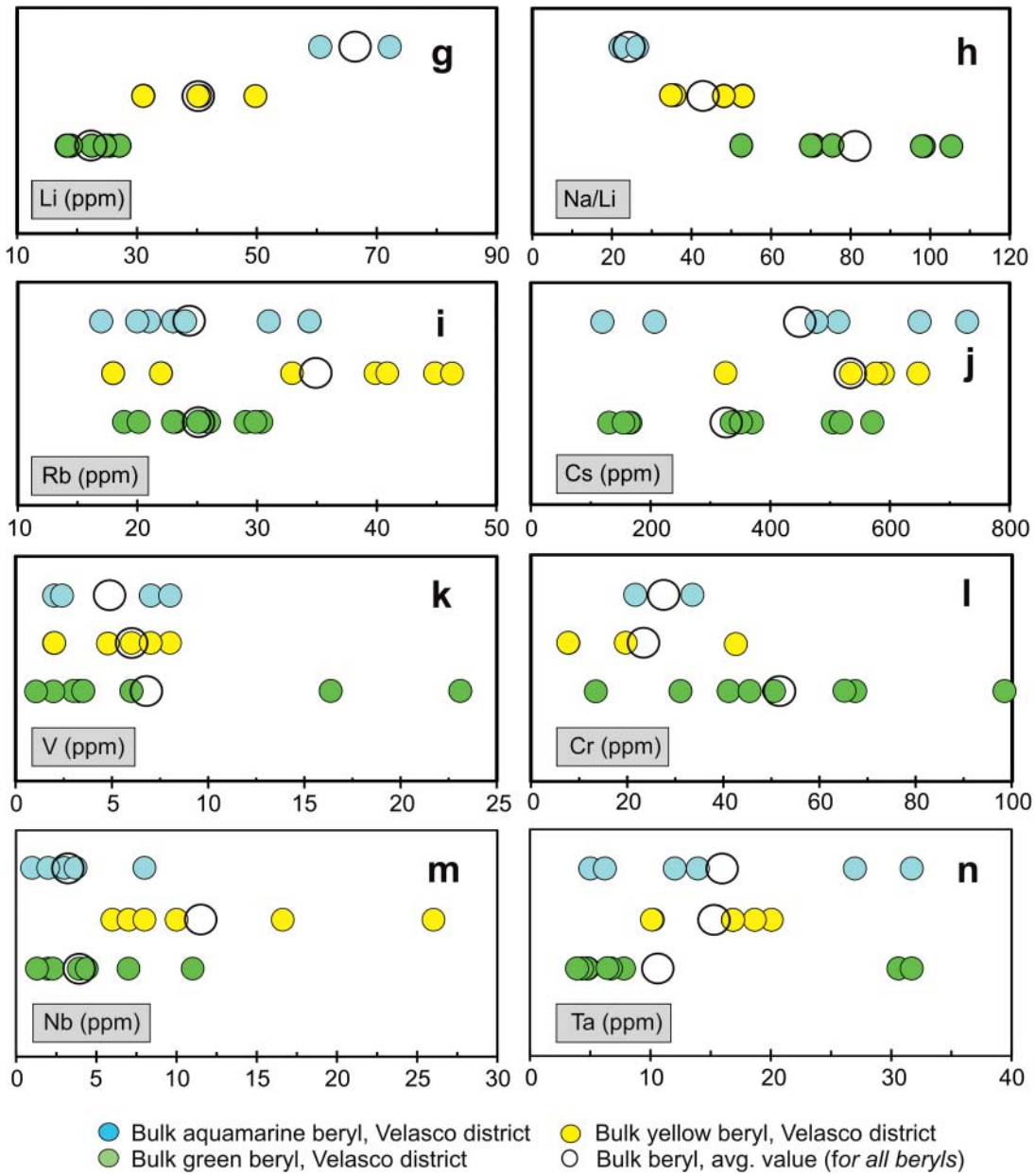

FIG. 3. Continued.

K^+, and Cs^+, and □ is a vacancy (*e.g.*, Aurisicchio *et al.* 2012).

Chemical variation of beryl and indicators of fractionation

Alkali elements and Fe–Mg behavior. Compositional variations of certain individual elements as well as relationships among elements in beryl can be indicators of fractionation and evolution of the pegmatites (*e.g.*, Černý 1975, Černý *et al.* 2003, Neiva & Neiva 2005). Among these elements, the alkali elements Li, Cs, and Na, and the ferromagnesian elements Fe and Mg are especially useful indicators of evolution (*e.g.*, Černý 1975, 2002, Aurisicchio *et al.* 1988, Černý *et al.* 2003, Neiva & Neiva 2005, Uher *et al.* 2010). Previous

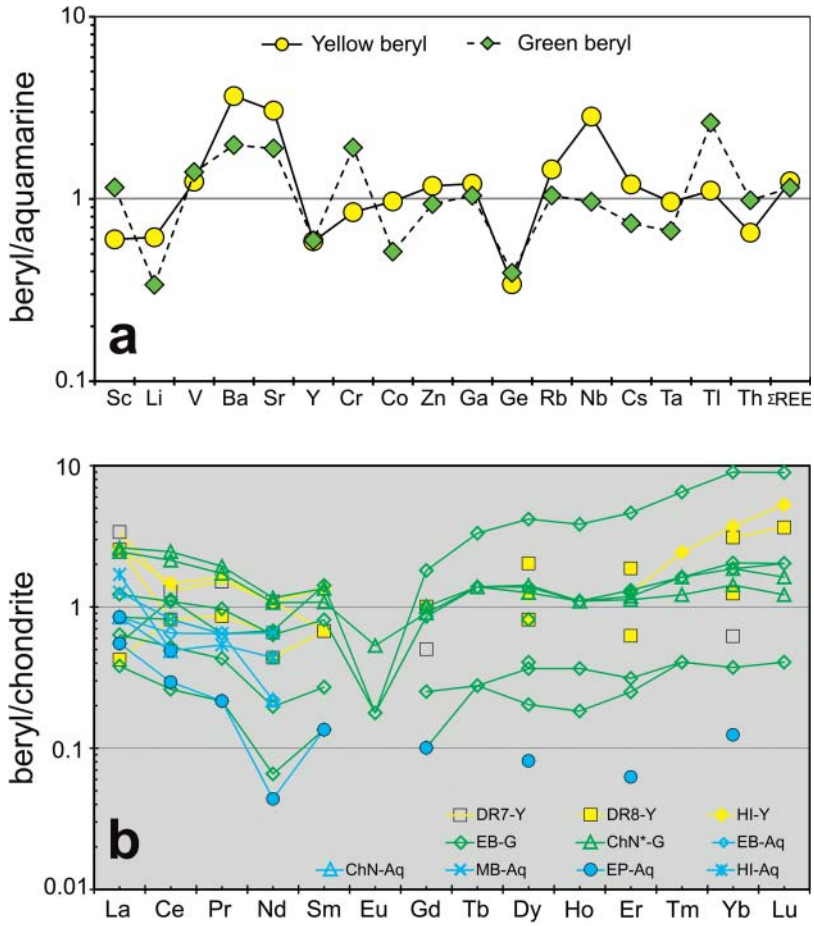

FIG. 4. (a) Spider diagram showing average values of yellow and green beryl normalized to the average aquamarine values. (b) Chondrite-normalized REE patterns of beryl from the Velasco district. Normalization values after McDonough & Sun (1995). Green, yellow, and blue symbols refer to green, yellow, and aquamarine beryl, respectively. In this and following figures, Y, G, and Aq after the abbreviation of each pegmatite name represent yellow, green, and aquamarine beryl, respectively. Pegmatite name abbreviations as in Table 1.

studies show that during fractionation, early beryl and the core of individual crystals tend to be enriched in ferromagnesian elements and depleted in alkali elements compared with late beryl and rims of individual crystals (*e.g.*, Trueman & Černý 1982, Černý 2002, Neiva & Neiva 2005, Wang *et al.* 2009, Aurisicchio *et al.* 2012). In beryl from the Velasco district Na dominates (0.02–0.45 wt.% Na_2O) over K (0.001–0.22 wt.% K_2O) and the relationship Na_2O/K_2O always exceeds unity (Tables 2, 3; Fig. 3d, e), which indicates that these are sodic beryl varieties according to the scheme of Černý (1975). Černý (1975) and Hawthorne & Černý (1977) assigned this type of beryl to pegmatites with albite-rich assemblages but very poor in rare alkalis.

In Figures 6 and 7 we present a series of diagrams to illustrate the geochemical evolution of beryl and the individual host pegmatites from the Velasco district. Because an increase in Li and Li+Cs correlates with an increase in Na from green beryl to yellow beryl and aquamarine (Fig. 6a, c, e), Na contents can be used as an indication of Li and Li+Cs contents in beryl samples for which Li contents are not available (EMP). The data set obtained by EMP generally shows that, overall, green beryl has slightly lower average Na contents compared to the rest (Figs. 6f; 3d). Yellow beryl has higher Na (and therefore Li) and lower Fe+Mg contents than green beryl (Figs. 3a, c, d; 6f). The plot of Fe+Mg *versus* Al for EMP compositions also shows that overall, green beryl tends to have the highest Fe +Mg contents and lowest Al contents compared with the rest, whereas yellow beryl, followed by aquamarine, has broad variations in Fe+Mg contents (Fig. 5). This

TABLE 4. UNIT-CELL DIMENSIONS OF BERYL FROM PEGMATITES, VELASCO DISTRICT, ARGENTINA

	Sample	*a* (Å)	*c* (Å)	V (Å^3)	*c/a*
Yellow Beryl	CH-Y	9.217	9.203	677.102	0.998
	DR8-Y	9.214	9.193	675.834	0.998
	DR8he-Y	9.213	9.196	675.955	0.998
	ChN-Y	9.210	9.198	675.692	0.999
	HI-Y	9.201	9.214	675.513	1.001
	Is-Y	9.198	9.217	675.327	1.002
	CV-Y	9.211	9.198	675.768	0.999
	DR8*-Y	9.217	9.199	676.749	0.998
	Min.	*9.198*	*9.193*	*675.327*	*0.998*
	Max.	*9.217*	*9.217*	*677.102*	*1.002*
	Avg.	*9.210*	*9.202*	*675.992*	*0.999*
Green Beryl	EB-G	9.212	9.193	675.593	0.998
	EB'-G	9.212	9.192	675.578	0.998
	ChN-G	9.202	9.216	675.779	1.002
	LE-G	9.213	9.193	675.662	0.998
	EB*-G	9.212	9.193	675.570	0.998
	EB*'-G	9.212	9.191	675.461	0.998
	EB*''-G	9.211	9.189	675.225	0.998
	EB*'''-G	9.213	9.189	675.371	0.997
	ChN*-G	9.213	9.190	675.508	0.998
	ChN*'-G	9.212	9.192	675.527	0.998
	HI*-G	9.210	9.188	674.891	0.998
	Min.	*9.202*	*9.188*	*674.891*	*0.997*
	Max.	*9.213*	*9.216*	*675.779*	*1.002*
	Avg.	*9.211*	*9.193*	*675.469*	*0.998*
Aquamarine	EB-Aq	9.201	9.217	675.735	1.002
	ChN-Aq	9.213	9.192	675.702	0.998
	MB-Aq	9.213	9.190	675.529	0.998
	HI-Aq	9.212	9.195	675.756	0.998
	EP-Aq	9.213	9.192	675.732	0.998
	EP*-Aq	9.213	9.192	675.777	0.998
	Min.	*9.201*	*9.190*	*675.529*	*0.998*
	Max.	*9.213*	*9.217*	*675.777*	*1.002*
	Avg.	*9.211*	*9.196*	*675.705*	*0.998*

Note: * Refers to powders that were chemically analyzed at IGME (Spain). Rest in ActLabs (Canada).

is not clear in the same plot using bulk beryl compositions, likely due to the small data set compared to that from EMP (Fig. A2b). Therefore, the lower Na contents in green beryl compared to yellow beryl also represent lower Li+Cs and Li contents in green beryl than in yellow beryl. The order of increasing Li, Na, and Cs contents and decreasing Na/Li ratios and Fe+Mg for all studied beryl from different pegmatites, as well as within single pegmatites, is green beryl → yellow beryl → aquamarine (Figs. 6a–f; 3g, h, j; 7a, b). Systematic changes in average Na/Li values are followed by a systematic variation in the relationship Na/Li *versus* Fe+Mg from mineral to mineral in the same order (Fig. 6b).

Within individual pegmatites, green beryl consistently has the lowest Li contents even though the Fe+Mg contents may not show a clear relationship in some cases (Figs. 6a–d, f; 7a). Therefore, the value of Fe+Mg alone is not the best indicator of relative evolution, but combined with Li, Na/Li, Na, Cs, and Li+Cs they show the evolution of beryl from least to most evolved (Figs. 7; 8a, b). All these color-composition relationships show a change from low to high degree of evolution from green to yellow beryl and finally aquamarine, and suggest that green beryl formed in the early stages of crystallization of the various pegmatites and incorporated less Li, Na, and Cs compared with yellow beryl and aquamarine,

TABLE 5. SUMMARY GEOLOGIC FEATURES OF GRANITIC PEGMATITES THAT CONTAIN GREEN, YELLOW, AND AQUAMARINE BERYL ANALYZED IN PREVIOUS STUDIES

Locality	Main & Accessory Minerals	Type of Pegmatite	Characteristics of Beryl, Location in Pegmatite	References
Beryller pegmatite, Salzburg, Austria	Qz, Mag, fl, Fap, zrn, Y& REE minerals	Pegmatite pods, 1 m. NYF	Blue: Quartz unit, up to 10 cm	Přikryl *et al.* (2014)
Bikita pegmatite, Zimbabwe	Li minerals, spd, lep, poll, ptl, tan, mclt, amblygonite	Giant, 1700 m long. Zoned. Petalite subtype, LCT[1]	Greenish, greenish to white: Wall zones	Černý *et al.* (2003)
Bratislava and Bojná massifs pegmatites, Central Western Carpathians, SW Slovakia	Ms, qz, Kfs, bt-chl, ghn, sp/wur, alm–sps, ferro col	Dikes or lenticular bodies. Zoned. Beryl type, beryl-columbite subtype	Pale green: On boundary between blocky Kfs zone and core	Uher *et al.* (2010)
Governador Valadares and Araçuai, Minas Gerais, Brazil	–	–	Dark blue to greenish blue: Wall and intermediate zones and pockets; < 5 cm long crystals; limpid, transparent, and commonly gem quality	Viana *et al.* (2002)
Greer Lake pegmatite group, Manitoba	Ab, Kfs, qz, clv, ms, grt, altered crd; rare pseudoixiolite, Li micas, mclt, ghn, rt, mnz, cst, zrn	Zoned	Greenish, yellowish: Intermediate zone, up to 2 × 10 cm Yellowish, bluish, or colorless: Core zone, up to 5 × 12 cm	
Itambé-Itapetinga area, Bahia, Brazil	Ms, or, grt, tur, col-tan, phenacite	Zoned	Yellow, green, and aquamarine, up to 10 cm	de Almeida Sampaio *et al.* (1973)
Koktokay #3 pegmatite, Altai District, China	elb-srl, ms, col, grt, spd, ambl, poll, elb, tant, mclt, Cs-lep	Zoned. Spodumene subtype, LCT family[1]	Greenish to yellowish green: Up to 5 cm (zone I). Greenish: In fine-grained albite, 0.5–1.5 × 1.5 to 4 cm (zone II). Green: 2 × 4 cm (zone III). Greenish: 3–5 × 6 to 8 cm (zone IV)	Wang *et al.* (2009)
Bonĕnov pegmatite, western Bohemia, Czech Republic	Ksp, ab, qz, grt, mag, fap, srl, ilm, mnz, xtm, zr, Nb, Ta, Ti oxides, rt, pcl	Dike, zoned, 5 m; beryl-columbite subtype. LCT	Yellow: External zone, up to 5 cm. Bluish green: Albite unit	Přikryl *et al.* (2014)
Kožichovice II pegmatite, Třebič, Czech Republic	Qz, ab, mc, ttn, Ce-aln, py, ilm, prt, Nb-rt, zrn, Ce-aeschynite, Nb-aeschynite, Y- and REE-rich vigezzite	Zoned. NYF	Pale green: Qz core, 3 cm	Novák & Filip (2010)
Masino-Bregaglia Massif, Italy	Grt, tur, rare minerals		Aquamarine, green-yellow, 15–20 cm	Bocchio *et al.* (2009)

TABLE 5. (CONTINUED)

Locality	Main & Accessory Minerals	Type of Pegmatite	Characteristics of Beryl, Location in Pegmatite	References
Mohave County, Arizona, USA	Fl, srl, ttn, grt, rare bt, ms	Zoned	Aquamarine: Border zone	Schaller *et al.* (1962)
Namivo pegmatite, Mozambique	Bt, ms, grt, tur, lep, spd, clv, tan-col, cookeite, bismutite	Concentrically zoned pegmatite. LCT?	Green: Most external zone, up to 9 × 6 cm and 5 × 2.3 cm	Neiva & Neiva (2005)
Oriental Pegmatite Province, Minas Gerais, Brazil	Ms, spd, petalite, cst, poll, tur, lpd, ambl	Generally zoned	Yellow, green, and aquamarine: Intermediate zone, some from core	Kahwage & Mendes (2003), Polli *et al.* (2006)
Quadeville, Ontario, Canada	Aln, fl, Fsrl, eux, gdl, mnz, col, ilm, grt, hem, zrn, py	Dike, zoned. 15 × 100 m. NYF	Dark greenish blue: Wall zone, 7 cm	Přikryl *et al.* (2014)
SD-2 pegmatite, Punilla district, Pampeana Pegmatite Province, Argentina	Ms, mc, bt, qz, fap, xtm, grt, fl, rt, hem, col group mins., pcl, mlc, mottramite, ccl, clays	Zoned. Rare-element class, beryl-columbite subtype; likely hybrid LCT-NYF	Intense yellow: Intermediate zone. Light green: External intermediate zone. Very light blue aquamarine: Wall zone	Colombo & Lira (2006)
Tanco pegmatite, Manitoba, Canada	Ms, qz, ab, spd, amb, lpd, Li-ms, poll	Zoned. Petalite subtype, LCT family[1,2]	Greenish to whitish: Wall zone	Černý & Simpson (1977)
Val Sissone, Central Alps, Italy	Qz, Kfs, ab, bt, ms, mag, chl, danalite, py, phenakite	Zoned. LCT	Blue: Central part, 3 cm	Přikryl *et al.* (2014)
Various localities (see other columns)	–	–	Yellow: Fort victoria field, Zimbabwe. Pale green: Jos, Nigeria. Aquamarine: Karoi, Zimbawe; Mursinka, Russia; Nuristan, Afghanistan; Isola d'Elba, Italy; Salinas mine, Minas Gerais, Brazil	Aurisicchio *et al.* (1988)
Various localities (see other columns)	Ab-ms-qz	–	Yellow (transparent honey-color): Replacement zone. Kaatiala pegmatite, Finland. Green: Cherlovaya Gora, East Baikal, Russia; Russia; Kaatiala pegmatite, Finland. Aquamarine:	Deer *et al.* (1997)

TABLE 5. (CONTINUED)

Locality	Main & Accessory Minerals	Type of Pegmatite	Characteristics of Beryl, Location in Pegmatite	References
			Boolcoomata, South Australia; C. Mondei, Montescheno, Italy; Brazil; Maxixe mine, Piauhy district, Mina Gerais, Brazil	
Zealand Station, New Brunswick, Canada	Ms, rt, cal, mnz, zm, ap, xtm	Dikes up to ~ 50 × 2 m	Aquamarine: Clear to milky, light to medium blue, up to 8 cm	Beal & Lentz (2010)

References in the Table are for sources of data. For pegmatite types: [1] Černý (1992), [2] Stilling *et al.* (2006). Mineral abbreviations: Albite – Ab, Almandine – Alm, Allanite – Aln, Amblygonite – Amb, Apatite – Ap, Biotite – Bt, Calcite – Cal, Cassiterite – Cst, Chrysocolla – Ccl, Cleavelandite – Clv, Chlorite – Chl, Columbite – Col, Cordierite – Crd, Elbaite – Elb, Euxenite – Eux, Ferrocolumbite – Ferro col, Fluorite – Fl, Fluorapatite – Fap, Fluorschorl – Fsrl, Gadolinite – Gdl, Gahnite – Ghn, Garnet – Grt, Hematite – Hem, Ilmenite – Ilm, K-feldspar – Kfs, Lepidolite – Lpd, Magnetite – Mag, Malachite – Mlc, Microcline – Mc, Microlite – Mclt, Monazite – Mnz, Muscovite – Ms, Orthoclase – Or, Petalite – Ptl, Pollucite – Poll, Pseudorutile – Prt, Pyrite – Py, Pyrochlore – Pcl, Quartz – Qz, Rutile – Rt, Sphalerite – Sp, Spodumene – Spd, Spessartine – Sps, Schorl – Srl, Tantalite – Tan, Titanite – Ttn, Tourmaline – Tur, Triplite – Trp, Wurtzite – Wur, Xenotime – Xtm, Zircon – Zrn. Very rare minerals not abbreviated.

which have the highest Li, Na, and Cs contents and the lowest Na/Li ratios, which is consistent with indicators of evolution obtained in previous studies (*e.g.*, Černý 2002, Černý *et al.* 2003).

A consistent change in the parameters Fe+Mg, Li, and Li+Cs, which measure degree of evolution (*e.g.*, Černý *et al.* 2003), seen in general among different pegmatites as well as within individual pegmatites, can be attributed to a compositional variation of the pegmatitic melt in individual bodies. Processes that can decrease and increase the parameters Fe+Mg and Li+Cs, respectively, include melt fractionation, crystallization of other mineral phases that host these elements (*i.e.*, micas, Fe-rich phosphates, other beryl), and reactions with host rocks during evolution (*e.g.*, Uher *et al.* 2010, Aurisicchio *et al.* 2012). However, the host rocks of the studied pegmatites are granitoids and there are no signs of interaction between the pegmatites and enclosing granites. Thus, assimilation cannot account for the observed compositional variations. Muscovite is present in all the studied pegmatites but it is a later phase compared with beryl and it would not have caused a change in the fractionating melt during crystallization of beryl. Iron-Mn phosphates (triplite) are present in most of the studied pegmatites. Therefore, crystallization of Fe-Mn phosphates and earlier beryl varieties during fractional crystallization likely account for the slight decrease in Fe+Mg and increase in Li and Cs in beryl varieties within individual pegmatites.

The relative evolution of pegmatitic melts can be inferred from the Na/Li *versus* Cs relationship in beryl (Trueman & Černý 1982, Černý 2002). Beryl from the Velasco district is characterized by low Cs contents and high Na/Li ratios (Fig. 8b) and falls within the "A" field for barren and geochemically primitive beryl-type pegmatites in the original Na/Li *versus* Cs diagram of Trueman & Černý (1982) and Černý (2002) (Fig. 8c). The pegmatites from the Velasco district were classified as beryl-columbite-phosphate subtype based on mineralogy (Galliski 1994a), which in the Na/Li *versus* Cs diagram of Černý (1975) and Černý (2002) falls in the "B" field of geochemically evolved beryl-columbite and beryl-columbite-phosphate pegmatites. However, based on the relationship between these parameters in beryl, the pegmatites from the Velasco district are characterized by a low degree of evolution.

Rb and Tl behavior in beryl. The relationship between Rb and Tl has been used in previous studies to understand the relative fractionation of some pegmatite minerals because Tl seems to follow the same order of preference as Rb (biotite > muscovite > K-feldspar; *e.g.*, Černý *et al.* 1985). However, Tl and Rb concentrations in beryl are one to two orders of magnitude lower than in muscovite and K-feldspar (Černý *et al.* 1985). For example, in the highly evolved Tanco pegmatite, Rb contents in K-feldspar and muscovite attain ~5.0 wt.% Rb, whereas beryl has only up to

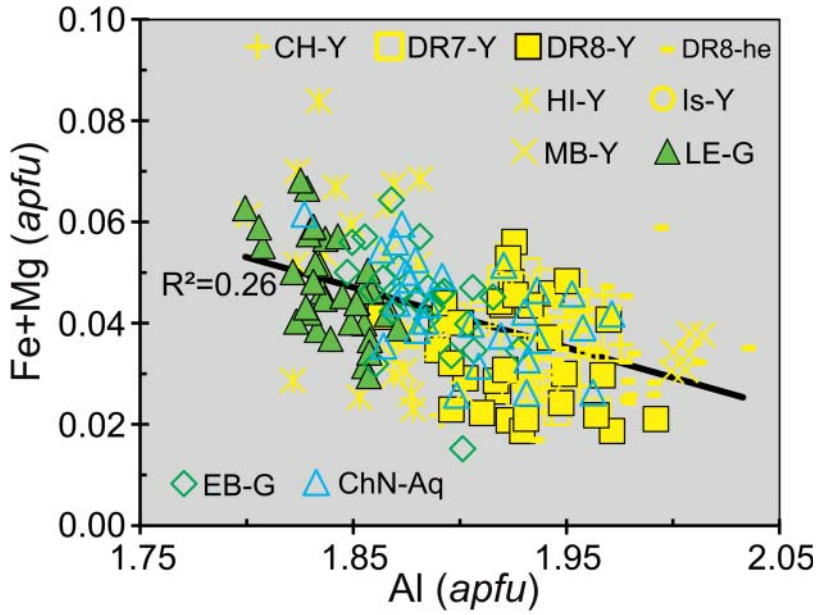

FIG. 5. Diagram showing a substitution operating in beryl from the Velasco district, Argentina. Fe+Mg (*apfu*) *versus* Al (*apfu*) for individual crystals by EMP analysis. Values based on 18 oxygen atoms *pfu*.

~0.1 wt.% Rb (Černý & Simpson 1977, Černý *et al.* 1985; Fig. 8a). For the Tanco pegmatite, the concentrations of Rb and Tl in beryl increase from early to late beryl and Rb/Tl slightly decreases with increasing Cs content (Černý & Simpson 1977, Černý *et al.* 1985). The Rb/Tl ratios may be similar in K-feldspar and micas as in beryl, as for example, in the Tanco and Altai No. 3 pegmatites (~65–300; Solodov 1962, Černý *et al.* 1985). Beryl from the Velasco district has much lower Rb (< 46 ppm) and Tl (< 1.2 ppm) contents compared to that in the Tanco and Altai No. 3 pegmatites, but it has a relatively wide range of Tl contents (~0.1–1.2 ppm; Fig. 8a). Overall, green beryl has lower Rb contents and lower Rb/Tl values than yellow beryl. However, in contrast with the observations at Tanco, no clear consistent trend can be seen among different varieties of beryl within individual pegmatites, and in some cases the Rb-Tl relations are inconsistent with the information gained from the more reliable indicators of evolution for beryl (Figs. 6–8). In any case, the extremely low Rb content in beryl is consistent with a very low degree of evolution for the Velasco pegmatites compared to the Tanco and Altai No. 3 pegmatites.

Al-Ga relationships in beryl. The behavior of Al and Ga was previously investigated for some minerals from the highly evolved Tanco pegmatite, the most Ga-enriched pegmatite, but the understanding of the fractionations measured was considered unsatisfactory (Černý *et al.* 1985). Some studies have analyzed the Ga content of beryl and found high concentrations, for example in that from the Sebago pegmatite, Maine, with up to 79 ppm Ga (Wise & Brown 2010). The orders of magnitude higher Ga contents (<100 ppm Ga) and lower Al/Ga ratios (<3,000) in Tanco beryl (Černý *et al.* 1985) than in Velasco beryl (18.5–31 ppm Ga; Al/Ga = 3,031–5,269; Fig. 8b) are consistent with beryl from the latter reflecting a very low degree of fractionation of the pegmatites (Fig. 8b). However, the relationship between Al/Ga and Ga is not a useful indicator of relative evolution of beryl varieties among or within Velasco district pegmatites because the aquamarine sample with the highest measured Cs and Li contents and some of the lowest Fe+Mg values has the highest Al/Ga ratio and lowest Ga contents, which is inconsistent with high Ga contents indicating advanced evolution (Fig. 8b).

Rare earth elements in beryl. Beryl does not incorporate REEs in large amounts, as exemplified by beryl from the Velasco district, in which the sum of REEs does not exceed 2.8 ppm (Tables 2, A3), and REE studies of beryl are very limited. However, in a study of beryl from the large and highly fractionated Namivo pegmatite in Mozambique, Neiva & Neiva (2005) showed that the concentrations of REEs in beryl increase from the external zone to the late core of the pegmatite, which suggests that REEs in beryl can provide information about the evolution of the crystallizing melt.

The general REE patterns of beryl from the Velasco district are somewhat similar to those obtained

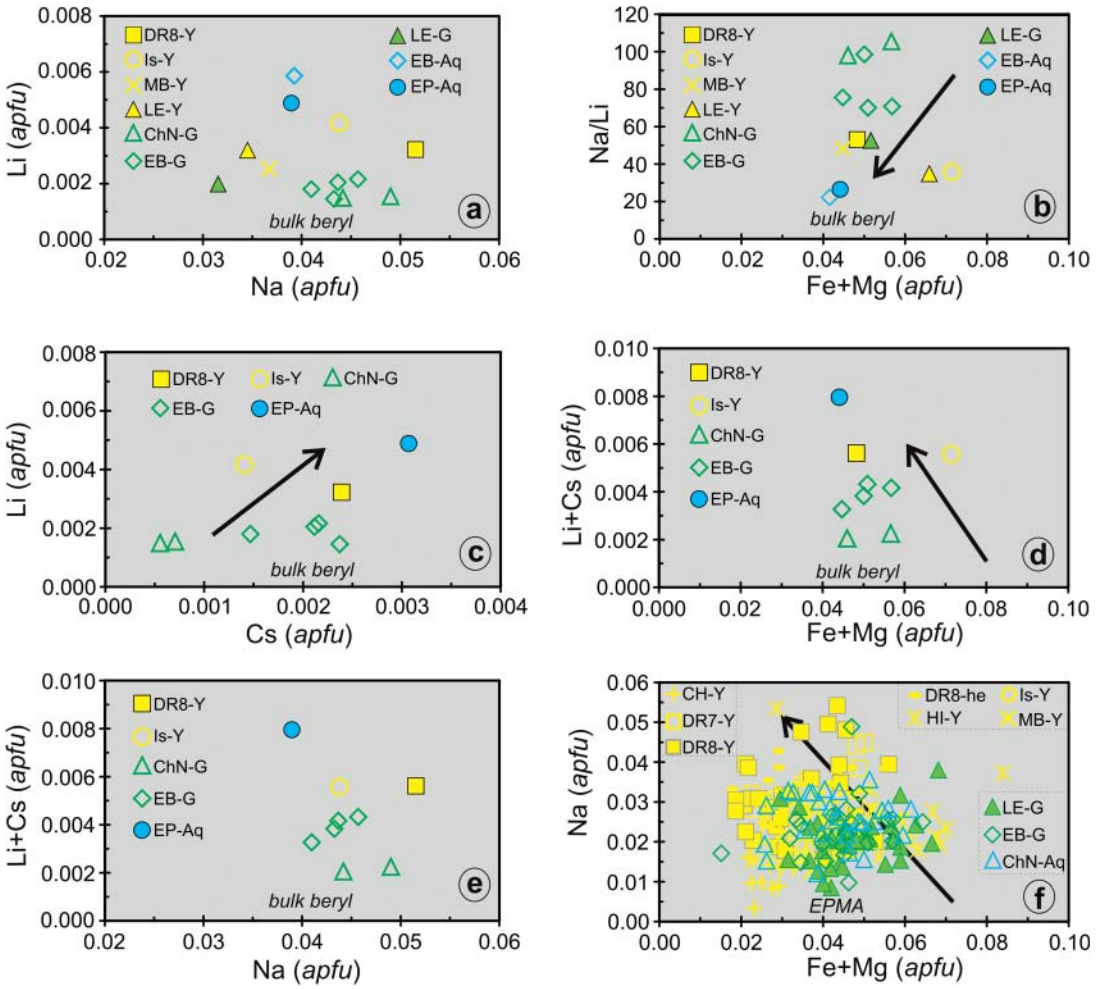

FIG. 6. Binary diagrams showing the fractionation characteristics of beryl from the Velasco district based on alkali and ferromagnesian element contents obtained from bulk beryl (a–e) and individual crystals by EMP (f). Values are in *apfu* for 18 oxygen atoms. (a) Li *versus* Na. (b) Na/Li *versus* Fe+Mg. Na/Li calculated from ppm. (c) Li *versus* Cs. (d) Li+Cs *versus* Fe+Mg. (e) Li+Cs *versus* Na. (f) Na *versus* Fe+Mg. A systematic change in the chemistry of beryl in the order green beryl → yellow beryl → aquamarine is observed. Arrows show the direction of evolution.

by Neiva & Neiva (2005), except for the middle REE enrichment they obtained for some beryl, which is not present in beryl from the Velasco district (Figs. 4b, A3). Beryl from the Velasco district also has patterns characterized by slightly decreasing light REE (LREE) contents from La to Sm, strong negative Eu anomalies that are also smaller than those from Mozambique, and slightly increasing heavy REE (HREE) contents from Eu to Lu (Figs. 4b, A3). In contrast, beryl from the Namivo pegmatite has decreasing HREEs from Gd to Lu. The strong negative Eu anomalies in Velasco district beryl are likely the result of the incorporation of Eu into plagioclase. In general, aquamarine has the lowest REE content of all beryl analyzed from the Velasco district, with generally low LREE contents and most HREEs below detection limits (Figs. 4b, A3). The aquamarine beryl with the highest Cs contents, reflecting a high degree of evolution, has the lowest REE contents of all beryl crystals analyzed. In addition, for individual pegmatites from the Velasco district for which data are available for different types of beryl, the total amount of REEs do not vary consistently between yellow and green beryl and aquamarine (Tables 2, A3; Figs. 4b, A3). Considering the alkali elements as good indicators of relative evolution in beryl, the finding that late beryl (aquamarine) is poor in REEs compared to early-formed beryl (green and yellow) contrasts with

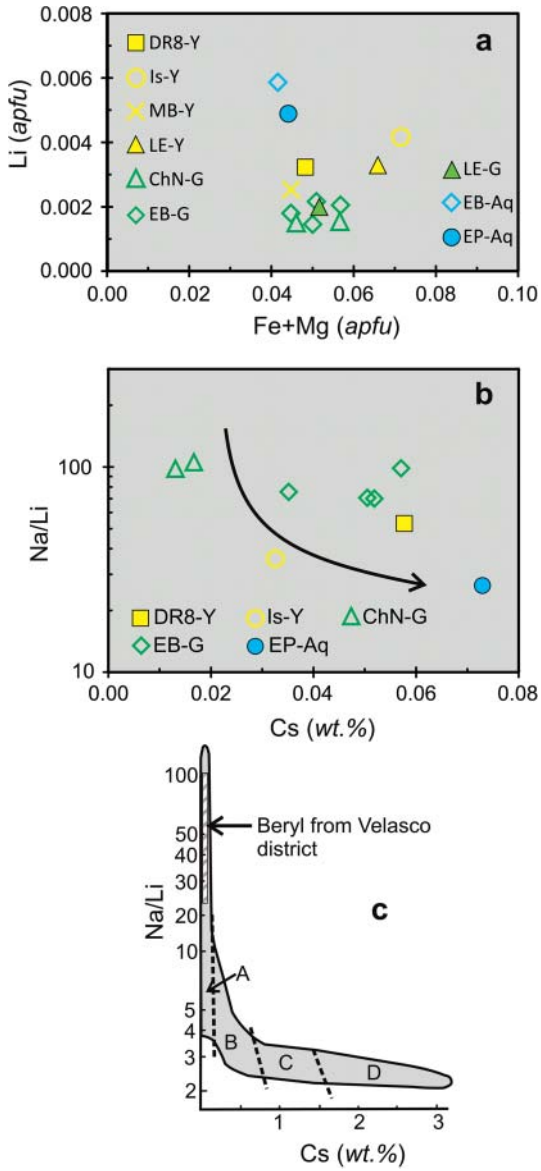

FIG. 7. Fractionation characteristics of beryl from the Velasco district. (a) Li *versus* Fe+Mg. Values in *apfu* (18 oxygen atoms). (b) Na/Li *versus* Cs (wt.%). After Černý (1975) and Černý (2002). Arrow is in the direction of evolution. (c) Same as (b) but showing the composition of beryl from the Velasco district and the fields defined by Černý (1975). Letters refer to: A. Sterile pegmatites and geochemically primitive beryl-type pegmatites. B. Beryl-columbite-type pegmatites and geochemically evolved beryl-columbite-phosphate pegmatites. C. Albite-spodumene and complex pegmatites. D. Highly fractionated Li, Cs, Ta-rich complex pegmatites. Na/Li calculated from ppm values.

the study of green, blue, and pink beryl from Mozambique by Neiva & Neiva (2005) in which REEs in beryl increase towards the center of the pegmatite. Our study suggests that fractional crystallization produced a decrease in the REE contents of the pegmatitic melt, consistent with other studies (*e.g.*, Morteani *et al.* 1995).

Finally, the abundance of HREEs and REEs in the different types of beryl varies: HREEs are higher in one type of beryl in some pegmatites and lower in others. Furthermore, the total REE contents of different crystals of the same color from the same pegmatite may be different (Fig. 4b), which may simply reflect changes in the fluid composition with crystallization of REE-bearing mineral phases such as apatite and perhaps muscovite. Therefore, our study shows that the total amount of REEs in beryl alone may not be a good indicator of fluid evolution and fractionation. What is more, these results point to the need for further detailed studies to fully understand the behavior of REEs in pegmatitic beryl.

Beryl composition and relative pegmatite evolution in the velasco district. El Bolsoncito and El Principio pegmatites, which have the highest Li and Cs contents, lowest Na/Li ratios, and among the lowest Fe+Mg contents (in aquamarine) among all studied samples of beryl, reflect the highest degree of evolution among the studied pegmatites from the Velasco district (Figs. 6, 7a,b). Based on the lowest Li and Cs (and Rb) contents and highest Na/Li ratios among all beryl samples analyzed, the lowest degree of evolution is inferred for the Chivo Negro pegmatite (Figs. 7b, 8a). We note that, because aquamarine is not present in all the pegmatites, a comparison between the compositions of beryl of different colors in a given pegmatite is used to evaluate the fractionation of the melt, which is not ideal, as the best indicator would be to compare beryl of similar color from each pegmatite.

Relationship color-composition in beryl

Based on a compilation from various studies, Černý (2002) determined that pure beryl is colorless, emerald (transparent green beryl) is due to the presence of Cr and/or V at the octahedral site, yellow beryl is due to Fe^{2+} in the channels, and different proportions of Fe^{2+}/Fe^{3+} correspond to green, yellow, or blue varieties. Other studies suggest that the color of beryl is dictated by the relative proportion of Fe^{3+} at the octahedral site (bluish) and of Fe^{2+} in the channels (*e.g.*, Viana *et al.* 2002, Beal & Lentz 2010), a decrease in the Fe^{3+}/Fe^{2+} ratio from green to bluish green to rose beryl (Neiva & Neiva 2005), and intervalence charge-transfer between Fe^{2+} and Fe^{3+} cations (*e.g.*, Taran & Rossman 2001, Anderson 2013). Groat *et al.*

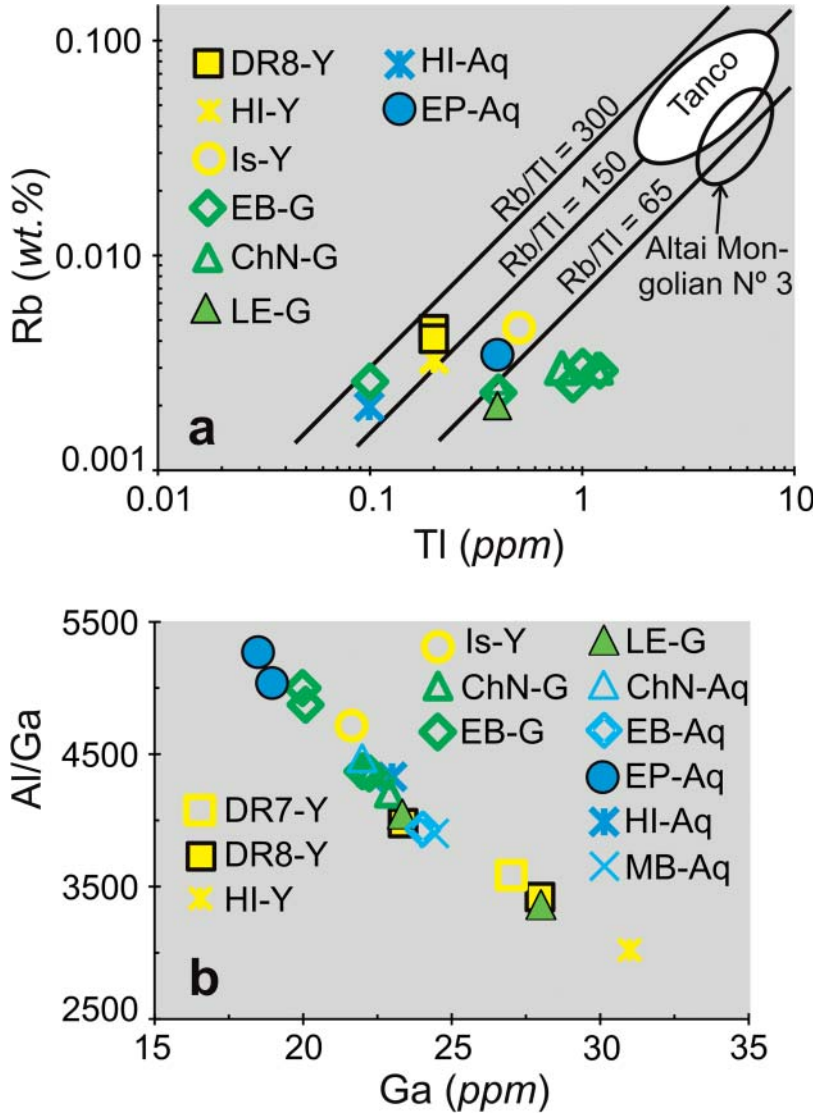

FIG. 8. Diagrams showing the chemistry of rare trace elements in beryl from the Velasco district. (a) Rb (wt.%) *versus* Tl (ppm), compared with the evolved Tanco and Altai Mongolian No. 3 pegmatites. After Černý *et al.* (1985), including data for beryl from the Tanco and Altai Mongolian pegmatites. (b) Al/Ga *versus* Ga (ppm).

(2010) used a variety of techniques to suggest that the blue color stems from intervalence charge transfer between Fe ions at the Al site and approximately 0.04 atoms per formula unit "excess" Fe at the 6*g* position, which is normally empty. Lin *et al.* (2013) used additional technqiues which confirmed this hypothesis. More recently, Přikryl *et al.* (2013) inferred that green beryl and bluish green beryl and blue beryl correspond to the presence or absence of Fe^{2+} at the *T2* site (Be tetrahedra), respectively. A color variation from green or bluish green to rose beryl was attributed to an increase in the Mn/Fe ratio (Neiva & Neiva 2005).

In our study of beryl from the Velasco district we have not measured the relative amounts of Fe^{2+} and Fe^{3+}. We have considered the elements that show significant concentration differences among beryl types. Of the elements investigated, the highest Cr contents were measured in green beryl, whereas yellow beryl and aquamarine have lower contents, which is consistent with Cr being a chromophore element responsible for

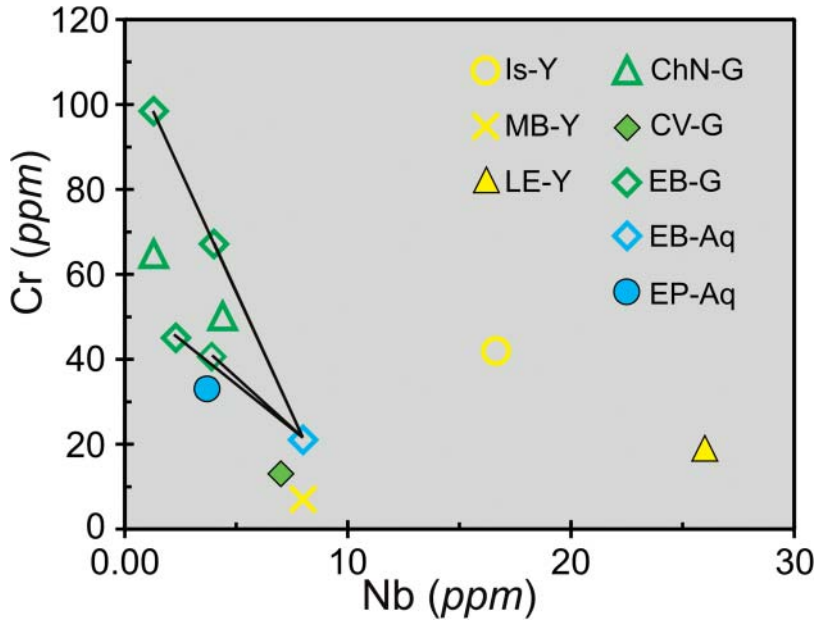

FIG. 9. Diagram showing elements that allow the separation of beryl types. Cr (ppm) *versus* Nb (ppm) (bulk beryl). Green beryl tends to have higher Cr and lower Nb contents than yellow beryl. Tie lines join beryl from the same pegmatite.

the green color of beryl (Černý 2002) (Figs. 3l, 4a, 9, A4). More importantly, within two individual pegmatites for which we have measured Cr in beryl of different colors, its content decreases in the order green beryl → yellow beryl and green beryl → aquamarine (Figs. 9, A4). Total iron contents in these beryl samples do not vary consistently among different beryl varieties. Because Cr tends to enter the structure of early-formed minerals, these findings are consistent with earlier observations about the evolution of the pegmatitic fluid in the Velasco district that indicate that in individual pegmatites green beryl precedes yellow beryl and aquamarine.

In addition to Cr, the relationship between Cr and Nb mark compositional differences between yellow and green beryl and aquamarine of the Velasco district, which may be promising indicators for separating beryl varieties in other pegmatites (Fig. 9). Overall, green beryl varieties have higher Cr and lower Nb contents than yellow beryl, which allows the separation of these two types of beryl in a graph of Cr *versus* Nb (Fig. 9). Aquamarine plots between these two types of beryl. Most importantly, the color-composition relationship is seen within individual pegmatites, where the Nb content increases from green to yellow beryl (Fig. 9). It is also evident from these relationships that Nb tends to concentrate in the late forms of beryl. We note that Nb has not been considered a chromophore element in previous investigations. Based on this study, Cr and Nb are good indicators of the compositional changes of the pegmatitic melt during fractionation as well as serving to distinguish beryl varieties. Further, this shows that the color of beryl is intimately linked to its composition and both are related to the evolution of the crystallizing melt.

Beryl unit-cell parameters and the structure-composition relationship

Unit cell parameter values (*a*, *c*, and *V*; Table 4) measured for beryl from the Velasco district are consistent with those obtained for similar beryl in previous studies (*e.g.*, de Almeida Sampaio *et al.* 1973, Aurisicchio *et al.* 1988, Černý *et al*. 2003, Neiva & Neiva 2005). Compared with beryl analyzed in previous studies, the most significant characteristic of beryl from the Velasco district is the low Li content and the small size of the unit-cell parameter *c* (<0.920 Å for most crystals; Fig. A1a). The values of the cell parameter *a* (9.201–9.217 Å) in beryl studied here are within the range measured for beryl worldwide, for example those from the Namivo pegmatite (Neiva & Neiva 2005) and the True Blue showing in the Yukon Territory (Groat *et al.* 2010). In contrast to what is observed for many beryl examples worldwide, there is no systematic change in the size of the unit cell parameters *a* and *c*, and the *c/a* ratio and the *c* parameter remain almost constant with greater amounts of Li substituting for Be at the tetrahedral

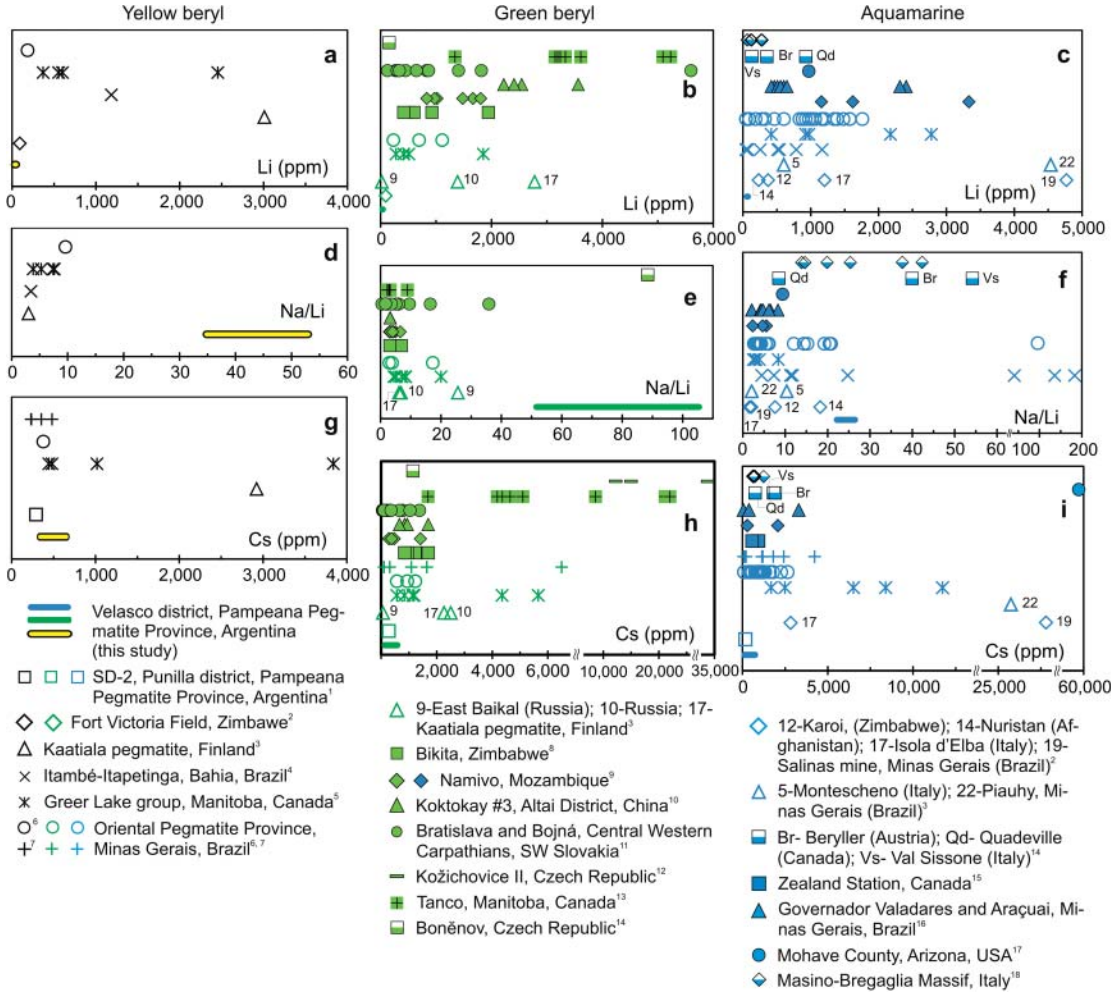

FIG. 10. Chemistry of yellow, green, and aquamarine beryl from the Velasco district compared to previously published pegmatitic beryl. (a, b, c) Li (ppm). (d, e, f) Na/Li (from ppm). (g, h, i) Cs (ppm). Sources of data as follows: 1 Colombo & Lira (2006), 2 Aurisicchio *et al.* (1988), 3 Deer *et al.* (1997), 4 De Almeida Sampaio *et al.* (1973), 5 Černý & Turnock (1975), 6 Kahwage & Mendes (2003), 7 Polli *et al.* (2006), 8 Černý *et al.* (2003), 9 Neiva & Neiva (2005), 10 Wang *et al.* (2009), 11 Uher *et al.* (2010), 12 Novák & Filip (2010), 13 Černý & Simpson (1977), 14 Přikryl *et al.* (2014), 15 Beal & Lentz (2010), 16 Viana *et al.* (2002), 17 Schaller *et al.* (1962), 18 Bocchio *et al.* (2009).

site (Fig. A1a), divalent cations (Fe+Mg) entering the octahedral position (Fig. A1b), and large alkali ions (Na+K+Rb+Cs) entering the channels (Fig. A1c). The fact that the *c/a* and the *c* parameters do not systematically change with Li contents, in contrast to what is seen in the evolved Namivo pegmatite (Neiva & Neiva 2005), is likely due to the extremely low Li and alkali content in the former, which tend to increase the size of the unit cell. The incorporation of Fe+Mg in place of Al at the octahedral site is not as limited and this explains the more 'normal' size of the *a* parameter. Therefore, the relationships between unit-cell parameter size and chemical compositions in beryl from the Velasco district reflect the limited evolution of the pegmatitic melt and its derived beryl.

Comparison with pegmatitic beryl worldwide and relative pegmatite evolution

To understand the relative evolution of the pegmatites as recorded by beryl, the chemical composition of yellow, green, and aquamarine beryl from the Velasco district was compared with beryl of similar colors from pegmatites worldwide (Table 5; Figs. 10, A5–A7). A summary of the main significant differences is presented here.

Alkali contents in beryl from the Velasco district reflect an extremely low degree of melt evolution compared with pegmatitic beryl worldwide (Figs. 10, A5–A7). Lithium, Cs, and Na contents are among the lowest measured in pegmatitic beryl of similar colors worldwide and similar to those in beryl from pegmatites in the Czech Republic, Italy, and Punilla district (Argentina) (Colombo & Lira 2006, Bocchio *et al.* 2009, Přikryl *et al.* 2014). For example, the highest Li (72 ppm), Cs (730 ppm), and Na_2O (0.45 wt.%) contents in beryl (aquamarine) from the Velasco district are orders of magnitude lower than those measured in aquamarine from the Greer Lake group pegmatites, Manitoba (<2,788 ppm Li, <~11,000 ppm Cs; Černý & Turnock 1975) and greenish beryl from the wall zone of the Tanco pegmatite (<2,000 ppm Li, <2.4 wt.% Cs_2O; 1.8 wt.% Na_2O; Černý & Simpson 1977) (Figs. 10, A5–A7). The highest Li content (4,768 ppm Li) reported so far in aquamarine corresponds to the Salinas pegmatite in Minas Gerais, Brazil (Aurisicchio *et al.* 1988). Rubidium contents in beryl from the Velasco district, however, are similar to or higher than in some beryl with high Li contents in the Bratislava and Bojna pegmatites (Uher *et al.* 2010), and lower than those in the evolved pegmatites from the Czech Republic (Novák & Filip 2010) that have the highest Rb contents (~1,500 ppm) of all similar beryl worldwide (Figs. A5f, A6f, A7f). This confirms our earlier observation that Rb contents in beryl may not best reflect pegmatitic fluid evolution in poorly evolved pegmatites.

The Na/Li relationship is higher in yellow and green beryl compared to all other beryl of similar colors worldwide, except for green beryl from the poorly evolved Czech Republic pegmatites that has a value close to the high end (Přikryl *et al.* 2014), reflecting the low degree of evolution of the pegmatites (Fig. 10d–f). For aquamarine, which has the lowest Na/Li ratios (Na/Li = 22; based on ppm) and reflects the highest degree of evolution of all beryl analyzed in this study, only some beryl from Bahia, Brazil (de Almeida Sampaio *et al.* 1973), one aquamarine from Minas Gerais, Brazil (Kahwage & Mendes 2003), and some aquamarine from poorly evolved pegmatites from Austria and Italy (Přikryl *et al.* 2014) have higher Na/Li ratios (Na/Li > 30) than those from the Velasco district. Beryl from the pegmatites from Bahia and Minas Gerais have wide compositional ranges but the great majority have low Na/Li ratios (< 20), and the latter coexists with Li-rich minerals (Table 5), which reflect a higher degree of evolution than in the Velasco district. Beryl from the Velasco district pegmatites studied here is either not spatially associated with Li-bearing minerals or they are extremely scarce and difficult to find (*e.g.*, Ricci 1971, Cravero 2005), which along with the Li/Na ratios demonstrates that beryl from the Velasco district reflects a lower degree of evolution than the Minas Gerais pegmatites.

Manganese contents in the green and yellow beryl studied here attain higher values than those in beryl from other pegmatites, whereas in the studied aquamarine they fall within the range of other aquamarine worldwide and reach the lowest values in poorly evolved pegmatites from Canada (Figs. A5b, A6b, A7b; Přikryl *et al.* 2014). Magnesium contents in beryl fall towards the low end of Mg contents measured in pegmatitic beryl worldwide (Figs. A5c, A6c, A7c). Interestingly, beryl in some of the most evolved pegmatites, including the Kozichovice II pegmatite in the Czech Republic (Novák & Filip 2010), the Namivo pegmatite (Neiva & Neiva 2005), the Bratislava and Bojna pegmatites in Slovakia (Uher *et al.* 2010), and pegmatites from Governador Valadares and Araçuai, Minas Gerais, Brazil (Viana *et al.* 2002), has much higher Mg contents than beryl from the Velasco district and the highest Mg contents of beryl worldwide (up to 0.5 wt.% MgO; Figs. A5c, A6c, A7c). However, these contents are lower than in beryl from pegmatites of a lower degree of evolution from Austria, Canada, and Italy (Přikryl *et al.* 2014).

Of the pegmatites for which beryl data were compiled, the ones that reflect the highest degree of evolution of the pegmatitic fluid correspond to the Tanco pegmatite (Černý & Simpson 1977), the Koktokay No. 3 pegmatite, China (Wang *et al.* 2009), Minas Gerais pegmatites, Brazil (Deer *et al.* 1997, Aurisicchio *et al.* 1988, Viana *et al.* 2002), Kaatiala pegmatite, Finland (Deer *et al.* 1997), and the

Namivo pegmatite, Mozambique (Neiva & Neiva 2005) (Figs. 10, A5–A7). Beryl in these pegmatites contains up to ~1.6 wt.% Li_2O. Among the pegmatites with the highest Cs contents in beryl of similar colors as those studied here are pegmatites from the Czech Republic (~35,000 ppm Cs; Novák & Filip 2010), the Tanco pegmatite (~22,500 ppm Cs; Černý & Simpson 1977), a pegmatite from Arizona, USA (~60,000 ppm Cs; Schaller *et al.* 1962), pegmatites from Greer Lake, Canada (~11,000 ppm Cs; Černý & Turnock 1975), and the Salinas and Piauhy pegmatites, Minas Gerais, Brazil (~30,500 ppm Cs; Aurisicchio *et al.* 1988, Deer *et al.* 1997; Fig. 10a–c).

It is worth noting that the most evolved beryl, which occurs in the internal zones of the pegmatites, is commonly not yellow or green beryl or aquamarine, but tends to be rose, white, and colorless varieties (Černý & Simpson 1977, Černý *et al.* 2003, Neiva & Neiva 2005, Wang *et al.* 2009) that have much higher Li (1.85 wt.% Li_2O) and Cs (28,297 ppm Cs) contents and lower Na/Li ratios compared to the most evolved beryl from the Velasco district pegmatites and those mentioned above.

Only one pegmatite of those from which beryl data are available, a pegmatite from the Punilla district, also in the Pampeana Pegmatite Province (Colombo & Lira 2006), contains the three varieties of beryl investigated here. Elemental abundances in beryl suggest that this pegmatite has a similar degree of evolution as those from the Velasco district (Figs. 10, A5–A7).

Conclusions

The major and trace element compositions of green, yellow, and aquamarine varieties of beryl in the pegmatites of the Velasco district, Argentina, reflect compositional changes in the magmatic melts during crystallization. Lithium (< 72 ppm) is a very minor substitution for Be at the tetrahedral position, Fe+Mg substitute in small amounts for Al at the octahedral position, and Na (< 3,338 ppm) followed by limited Cs (< 730 ppm) predominate in the channels. The substitutions at the octahedral site, although minor, dominate over the tetrahedral site. A short *c* cell dimension and no systematic change in the size of the *a* and *c* unit cell parameters with variations in the amount of Li, alkalis, and Fe+Mg are due to the extremely low degree of substitution of Be by Li and the very limited incorporation of alkalis in the channels, which reflect the low degree of evolution of the pegmatites from the Velasco district.

The chromatic component that most influences the color of the studied beryl is Cr, with green beryl having the highest Cr contents. Within individual pegmatites, the Cr content is higher in green beryl than in yellow beryl and aquamarine. Green beryl is also characterized by higher Cr and lower Nb contents than yellow beryl, and this allows the separation of these types of beryl in a graph of Cr *versus* Nb. Thus, this study suggests that Cr and Nb are good indicators of the compositional changes of the pegmatitic fluid during fractionation and also help distinguish different types of beryl.

The relative evolution of beryl within and among the pegmatites from the Velasco district is well described by the alkali element contents (Li, Cs, Na) and the Na/Li ratios. A decrease in Na/Li ratios and Fe+Mg and an increase in Li and Cs in the order green beryl → yellow beryl → aquamarine within individual pegmatites, as well as among pegmatites, reflect the crystallization of green beryl during an early stage and yellow beryl and aquamarine during the latest stage of crystallization of the melt. Aquamarine from the El Principio and El Bolsoncito pegmatites has the highest Li and Cs contents, the lowest Na/Li ratios, and among the lowest Fe+Mg contents, reflecting the highest degree of fractionation among the studied pegmatites. The Chivo Negro pegmatite evidences the lowest degree of evolution based on the low Li and Cs contents and high Na/Li ratios in beryl.

In the poorly evolved beryl from the Velasco district the elements Rb and Tl, as well as the relationship Al/Ga, are not useful discriminators of relative evolution among the pegmatites. However, a comparison of Al/Ga ratios and Ga contents with those from highly evolved pegmatites shows that relatively higher Al/Ga ratios and lower Ga contents in beryl are typical of poorly evolved pegmatites such as those from the Velasco district. Aquamarine has the lowest REE content of all beryl analyzed from the Velasco district, which suggests that fractional crystallization produced a decrease in the REE contents of the pegmatitic melt.

Beryl from the Velasco district, in particular green beryl and aquamarine, is compositionally similar to beryl derived from pegmatites or external pegmatite zones characterized by a low degree of fractionation, and formed in a geochemical environment poor in alkaline elements. Compositionally, this beryl is similar to those from a pegmatite from the Punilla district, Argentina. Lithium contents in green, yellow, and aquamarine beryl from the Velasco district are the lowest measured in all pegmatitic beryl of similar colors worldwide, and the highest Li and Cs contents are orders of magnitude lower than those in similar beryl in highly evolved rare-element pegmatites from Minas Gerais (Brazil), the Tanco pegmatite, the Namivo pegmatite, the Koktokay No. 3 pegmatite, and the Kaatiala pegmatite (Finland).

Acknowledgements

Funding for this project was provided by ECU Thomas Harriot College of Arts and Sciences and

Research and Graduate Studies to AH. FS thanks Consejo Nacional de Investigaciones (CONICET, Argentina) for a postdoctoral scholarship to undertake the present study at East Carolina University (ECU), and the Department of Geological Sciences at ECU for hosting his postdoctoral stay. We are indebted to Richard Mauger for his help with the XRD and to Jim Watson and Richard Mauger for their help with mineral and rock crushing and mineral separation at ECU. Josh Bitner is thanked for providing transport to Fayetteville State University to FS. Nick Foster is thanked for assistance with EMP analysis and Tom Fink with SEM-EDS analysis. Careful and constructive reviews by Edward Grew and Milan Novák are greatly appreciated, as are comments by Associate Editor Pietro Vignola and suggestions and handling of the manuscript by Editor Lee Groat.

References

Alfonso, P., Melgarejo, J., Yusta, I., & Velasco, F. (2003) Geochemistry of feldspars and muscovite in granitic pegmatite from The Cap de Creus field, Catalonia, Spain. *Canadian Mineralogist* **41**, 103–116.

Anderson, L. (2013) The yellow color center and trapped electrons in beryl. *Canadian Mineralogist* **51**, 15–25.

Aurisicchio, C., Fioravanti, G., Grubessi, O., & Zanazzi, P. (1988) Reappraisal of the crystal chemistry of beryl. *American Mineralogist* **73**, 826–837.

Aurisicchio, C., Conte, M., De Vito, C., & Ottolini, L. (2012) Beryl from miarolitic pockets of granitic pegmatites, Elba, Italy: Characterization of crystal chemistry by means of EMP and SIMS analyses. *Canadian Mineralogist* **50**, 1467–1488.

Báez, M., Basei, M., Toselli, A., & Rossi, J. (2004) Geocronología de granitos de la sierra de Velasco (Argentina): reinterpretación de la secuencia magmática. *Simposio 40 anos de Geocronologia no Brasil*, 85.

Báez, M., Bellos, L., Grosse, P., & Sardi, F. (2005) Caracterización petrológica de la sierra de Velasco. *In* Geología de la provincia La Rioja (Precámbrico-Paleozoico inferior) (J. Dalhquist, E. Baldo, & P. Alasino, eds.). *Asociación Geológica Argentina, Serie D: Publicación Especial* **8**, 123–130.

Báez, M., Basei, M., Rossi, J., & Toselli, A. (2008) Geochronology of Paleozoic magmatic events in Northern Sierra de Velasco, Argentina. *VI South American Symposium on Isotope Geology*, CD-Proceeding, **Paper 17**, 5 pp.

Barton, M.D. & Young, S. (2002) Non-pegmatitic deposits of beryllium: mineralogy, geology, phase equilibria and origin. *Reviews in Mineralogy and Geochemistry* **50**, 591–691.

Beal, K. & Lentz, D. (2010) Aquamarine beryl from Zealand Station, Canada: a mineralogical and stable isotope study. *Journal of Geosciences* **55**, 57–67.

Bellos, L. (2008) *Petrología de los granitoides del sur de la Sierra de Velasco y su significación regional*. Ph.D. Thesis, Universidad Nacional de Córdoba (Argentina), 334 p.

Bocchio, R., Adamo, I., & Caucia, F. (2009) Aquamarine from the Masino-Bregaglia Massif, Central Alps, Italy. *Gems & Gemology* **45**, 204–207.

Bragg, W.L. & West, J. (1926) The structure of beryl. *Proceedings of the Royal Society London* **3A**, 691–714.

Černý, P. (1975) Alkali variations in pegmatitic beryls and their petrogenetic implications. *Neues Jahrbuch für Mineralogie-Abhandlungen* **123**, 198–212.

Černý, P. (1991) Rare-element granitic pegmatites. Part I: anatomy and internal evolution of pegmatite deposits & Part II: regional to global environments and petrogenesis. *Geoscience Canada* **18**, 49–81.

Černý, P. (1992) Geochemical and petrogenetic features of mineralization in rare element granitic pegmatites in the light of current research. *Applied Geochemistry* **7**, 393–416.

Černý, P. (2002) Mineralogy of beryllium in granitic pegmatites. *In* Beryllium: mineralogy, petrology and geochemistry (E. Grew, ed.). *Reviews in Mineralogy and Geochemistry* **50**, 405–444.

Černý, P. & Ercit, T. (2005) The classification of granitic pegmatites revisited. *Canadian Mineralogist* **43**, 2005–2026.

Černý, P. & Simpson, F. (1977) The Tanco pegmatite at Bernic Lake, Manitoba. IX Beryl. *Canadian Mineralogist* **15**, 489–499.

Černý, P. & Turnock, A. (1975) Beryl from the granitic pegmatites at Greer Lake, Southeastern Manitoba. *Canadian Mineralogist* **13**, 55–61.

Černý, P., Meintzer, R., & Anderson, A. (1985) Extreme fractionation in rare-element granitic pegmatites: selected examples of data and mechanisms. *Canadian Mineralogist* **23**, 381–421.

Černý, P., Anderson, A., Tomascak, P., & Chapman, R. (2003) Geochemical and morphological features of beryl from the Bikita granitic pegmatite, Zinbawe. *Canadian Mineralogist* **41**, 1003–1011.

Colombo, F. & Lira, R. (2006) Geología y mineralogía de algunas pegmatitas del borde oriental del distrito Punilla, Córdoba. *Revista de la Asociación Geológica Argentina* **61**, 393–407.

Cravero, O. (2005) Las pegmatitas zonadas de la sierra de Velasco, La Rioja. *Serie de Correlación Geológica* **19**, 133–144.

DAHLQUIST, J., PANKHURST, R., RAPELA, C., CASQUET, C., FANNING, C., ALASINO, P., & BÁEZ, M. (2006) The San Blas Pluton: An example of Carboniferous plutonism in the Sierras Pampeanas, Argentina. *Journal of South American Earth Sciences* **20**, 341–350.

DAHLQUIST, J., ALASINO, P., EBY, N., GALINDO, C., & CASQUET, C. (2010) Fault controlled Carboniferous A-type magmatism in the proto-Andean foreland (Sierras Pampeanas, Argentina): Geochemical constraints and petrogenesis. *Lithos* **115**, 65–81.

DE ALMEIDA SAMPAIO, H., SIGHINOLFI, G.P., & GALLI, E. (1973) Contribution to the crystal chemistry of beryl. *Contributions to Mineralogy and Petrology* **38**, 279–290.

DEER, W.A., HOWIE, R.A., & ZUSSMAN, J. (1997) Rock-forming minerals. Volume 1B, Disilicates and Ring Silicates. *The Geological Society of London*, 629 p.

EVENSEN, J.M. & LONDON, D. (2002) Experimental silicate mineral/melt partition coefficients for beryllium and the crustal Be cycle from migmatite to pegmatite. *Geochimica et Cosmochimica Acta* **66**, 2239–2265.

GALLISKI, M. (1994a) La Provincia Pegmatítica Pampeana. I: Tipología y distribución de sus distritos económicos. *Revista de la Asociación Geológica Argentina* **49**, 99–112.

GALLISKI, M. (1994b) La Provincia Pegmatítica Pampeana. II: Metalogénesis de sus distritos económicos. *Revista de la Asociación Geológica Argentina* **49**, 113–122.

GALLISKI, M. (2009) The Pampean Pegmatite Province, Argentina: a review. *Estudos Geológicos* **19**, 30–34.

GALLISKI, M., PERINO, E., GASQUEZ, J., MARQUEZ ZAVALÍA, M., & OLSINA, R. (1997) Geoquímica de feldespatos potásicos y muscovitas como guía de exploración de pegmatitas graníticas de algunos distritos de la provincia pegmatítica pampeana. *Revista de la Asociación Geológica Argentina* **52**, 24–32.

GIBBS, G.V., BRECK, D.W., & MEAGHER, E.P. (1968) Structural refinement of hydrous and anhydrous synthetic beryl and emerald: $Al_2Be_3Si_6O_{18}$, $Al_{1.9}Cr_{0.1}Be_3Si_6O_{18}$. *Lithos* **1**, 275–285.

GIULIANI, G., FRANCE-LANORD, C., ZIMMERMANN, J.L., CHEILLETZ, A., ARBOLEDA, C., CHAROY, B., COGET, P., FONTAN, F., & GIARD, D. (1997) Fluid composition, δD of channel H_2O, and $\delta^{18}O$ of lattice oxygen in beryls: genetic implications for Brazilian, Colombian, and Afghanistani emerald deposits. *International Geology Review* **39**, 400–424.

GONZÁLEZ-BONORINO, F. (1951) Una nueva formación Precámbrica en el noroeste Argentino. *Comunicación Científica, Museo de La Plata* **5**, 4–6.

GREW, E.S. (2002) Mineralogy, petrology and geochemistry of beryllium: an introduction and list of beryllium minerals. *Reviews in Mineralogy and Geochemistry* **50**, 1–76.

GROAT, L., ROSSMAN, G., DYAR, M., TURNER, D., PICCOLI, P., & SCHULTZ, A. (2010) Crystal chemistry of dark blue aquamarine from the True Blue Showing, Yukon Territory, Canada. *Canadian Mineralogist* **48**, 597–613.

GROSSE, P. & SARDI, F. (2005) Geología de los granitos Huaco y Sanagasta, sector centro-oriental de la Sierra de Velasco, La Rioja. *Serie de Correlación Geológica* **19**, 221–238.

GROSSE, P., SÖLLNER, F., BÁEZ, M., TOSELLI, A., ROSSI, J., & DE LA ROSA, D. (2009) Lower Carboniferous post-orogenic granites in central-eastern Sierra de Velasco, Sierras Pampeanas, Argentina: U-Pb monazite geochronology, geochemistry and Sr-Nd isotopes. *International Journal of Earth Sciences* **98**, 1001–1025.

HAWTHORNE, F. & ČERNÝ, P. (1977) The alkali-metal positions in Cs-Li beryl. *Canadian Mineralogist* **15**, 414–421.

HERRERA, A. (1965) Evolución geoquímica de las pegmatitas zonales de los principales distritos argentinos. *Revista de la Asociación Geológica Argentina* **20**, 199–228.

HERRERA, A. (1968) Geochemical evolution of zoned pegmatites of Argentina. *Economic Geology* **63**, 13–29.

HÖCKENRIENER, M., SÖLLNER, F., & MILLER, H. (2003) Dating the TIPA shear zone: Early Devonian terrane boundary between Famatinian and Pampean systems (NW Argentina). *Journal of South American Earth Sciences* **16**, 45–66.

ISOTANI, S., FURTADO, W., ANTONINI, R., & DIAS, O. (1989) Line-shape and thermal kinetics analysis of the Fe^{++} band in Brazilian green beryl. *American Mineralogist* **74**, 432–438.

KAHWAGE, M. & MENDES, J. (2003) O berilo gemológico da provincia pegmatitica Oriental do Brasil. *Geochimica Brasiliensis* **17**, 13–25.

LIN, J., CHEN, N., HUANG, D., & PAN, Y. (2013) Iron pairs in beryl: New insights from electron paramagnetic resonance and synchrotron X-ray absorption spectroscopy, and ab initio calculations. *American Mineralogist* **98**, 1745–1753.

LONDON, D. & EVENSEN, J.M. (2002) Beryllium in silicic magmas and the origin of beryl-bearing pegmatites. *Reviews in Mineralogy and Geochemistry* **50**, 445–485.

LÓPEZ, J.P., GROSSE, P., & TOSELLI, A. (2007) Faja de deformación La Horqueta, Sierra de Velasco, Sierras Pampeanas, NO de Argentina: petrografía, geoquímica, estructuras y significado tectónico. *Estudios Geológicos* **63**, 5–18.

MCDONOUGH, W. & SUN, S. (1995) The composition of the Earth. *Chemical Geology* **120**, 223–253.

MORTEANI, G., PREINFALK, C., SPIEGEL, W., & BONALUMI, A. (1995) The Achala granitic complex and the pegmatites of the Sierras Pampeanas (Northwest Argentina): A study of differentiation. *Economic Geology* **90**, 636–647.

NEIVA, A. & NEIVA, J. (2005) Beryl from the granitic pegmatite at Namivo, Alto Ligonha, Mozambique. *Neues Jahrbuch für Mineralogie-Abhandlungen* **18**, 173–182.

NOVÁK, M. & FILIP, J. (2010) Unusual (Na,Mg)-enriched beryl and its breakdown products (beryl II, bazzite, bavenite) from euxenite-type NYF pegmatite related to the orogenic ultrapotassic Třebíč pluton, Czech Republic. *Canadian Mineralogist* **48**, 615–628.

PANKHURST, R.J., RAPELA, C., & FANNING, M. (2000) Age and origin of coeval TTG, I- and S-type granites in the Famatinian belt of NW Argentina. *Transactions of the Royal Society of Edinburgh: Earth Sciences* **91**, 151–168.

POLLI, G., OLIVEIRA, E., SABIONI, A., FERREIRA, A., & ROESER, H. (2006) Análise da composição química em variedades de berilo, por ativação neutrônica instrumental (INAA). *Geochimica Brasiliensis* **20**, 191–207.

PŘIKRYL, J., NOVÁK, M., FILIP, J., GADAS, P., & VAŠINOVÁ, M.G. (2013) Iron-bearing beryl from granitic pegmatites; EMPA, LA-ICP-MS, Mossbauer spectroscopy and powder XRD study. *PEG 2013: The 6th International Symposium on Granitic Pegmatites, Abstracts*, 116–117.

PŘIKRYL, J., NOVÁK, M., FILIP, J., GADAS, P., & VAŠINOVÁ GALIOVÁ, M. (2014) Iron+Magnesium-bearing beryl from granitic pegmatites: An EMPA, LA-ICP-MS, Mössbauer spectroscopy, and powder XRD study. *Canadian Mineralogist* **52**, 271–284.

RAPELA, C., CASQUET, C., BALDO, E., DAHLQUIST, J., PANKHURST, R., GALINDO, C., & SAAVEDRA, J. (2001a) Las Orogénesis del Paleozoico inferior en el margen proto-andino de América del Sur, Sierras Pampeanas, Argentina. *Journal of Iberian Geology* **27**, 23–41.

RAPELA, C.W., PANKHURST, R.J., BALDO, E., CASQUET, C., GALINDO, C., FANNING, C.M., & SAAVEDRA, J. (2001b) Ordovician metamorphism in the Sierras Pampeanas: New U-Pb SHRIMP ages in Central-East Valle Fértil and the Velasco Batholith. *III Simposio Sudamericano de Geología Isotópica (III SSAGI)* Article **616**, 4 pp.

RICCI, H.I. (1971) Geología y evaluación preliminar de las pegmatitas de la sierra de Velasco, Departamento Capital, Sanagasta y Castro Barros. La Rioja. *Dirección Provincial de Minería, La Rioja, Informe inédito*, 50 pp.

SAADI, J. (2006) *Las piedras preciosas de la República Argentina*. Pugliese-Siena, Córdoba, Argentina, 183 pp.

SARDI, F.G. (2005) Petrografía y caracterización de la mena del distrito pegmatítico Velasco, La Rioja, Argentina. *XVI Congreso Geológico Argentino* **V**, 231–238.

SARDI, F.G. (2008) The geological context of gems in the Velasco Pegmatitic District, Argentina. *Journal of Gemmology* **31**, 85–89.

SARDI, F.G. & GROSSE, P. (2005) Consideraciones sobre la clasificación del distrito Velasco de la Provincia Pegmatítica Pampeana, Argentina. *XVI Congreso Geológico Argentino* **V**, 239–242.

SARDI, F., MURATA, M., & GROSSE, P. (2010) Petrographical and geochemical features of the granite-pegmatite transition in the Velasco Pegmatitic District, NW Argentina. *Neues Jahrbuch für Geologie und Palaöntologie* **258**, 61–71.

SCHALLER, W., STEVENS, R., & JAHNS, R. (1962) An unusual beryl from Arizona. *American Mineralogist* **47**, 672–699.

SHERRIFF, B., DOUGLAS GRUNDY, H., HARTMAN, S., HAWTHORNE, F., & ČERNÝ, P. (1991) The incorporation of alkalis in beryl: multi-nuclear MAS NMR and crystal-structure study. *Canadian Mineralogist* **29**, 271–285.

SOLODOV, N.A. (1962) Distribution of thallium among the minerals of a zoned pegmatite. *Geochemistry*, 738–741.

STILLING, A., VANSTONE, P., & ČERNÝ. P. (2006) The Tanco pegmatite at Bernic Lake, Manitoba. XVI. Zonal and bulk compositions and their petrogenetic significance. *Canadian Mineralogist* **44**, 599–623.

TARAN, M.N. & ROSSMAN, G.R. (2001) Optical spectroscopic study of tuhualite and a re-examination of the beryl, cordierite, and osumilite spectra. *American Mineralogist* **86**, 973–980.

TOSELLI, A., ROSSI, J., SARDI, F., LÓPEZ, J., & BÁEZ, M. (2000) Caracterización petrográfica y geoquímica de granitoides de la sierra de Velasco, La Rioja, Argentina. *17 Geowissenschaftliches Lateinamerika-Kolloquium (17 LAK)* **81**, 6 pp.

TOSELLI, A., ROSSI, J., MILLER, H., BÁEZ, M., GROSSE, P., LÓPEZ, J., & BELLOS, L. (2005) Las rocas graníticas y metamórficas de la Sierra de Velasco. *Serie de Correlación Geológica* **19**, 211–220.

TOSELLI, A., MILLER, H., ACEÑOLAZA, F., ROSSI, J., & SÖLLNER, F. (2007) The Sierra de Velasco (northwestern Argentina) – an example from polyphase magmatism at the margin of Gondwana. *Neues Jahrbuch fur Mineralogie-Abhandlungen* **246**, 325–345.

TRUEMAN, D.L. & ČERNÝ, P. (1982) Exploration for rare-element granitic pegmatites. *Mineralogical Association of Canada Short Course Handbook* **8**, 463–493.

UHER, P., CHUDÍK, P., BAĆÍK, P., VACULOVIČ, T., & GALIOVÁ, M. (2010) Beryl composition and evolution trends: an example from granitic pegmatites of the beryl-columbite subtype, Western Carpathians, Slovakia. *Journal of Geosciences* **55**, 69–80.

VERDECCHIA, S., BALDO, E., BENEDETTO, J., & BORGHI, P. (2007) The first shelly fauna from metamorphic rocks of the Sierras Pampeanas (La Cébila Formation, Sierra de Ambato, Argentina): age and paleogeographic implications. *Ameghiniana* **44**, 493–498.

VIANA, R., JORDT-EVANGELISTA, H., DA COSTA, M., & STERN, W. (2002) Characterization of beryl (aquamarine variety)

from pegmatites of Minas Gerais, Brazil. *Physics and Chemistry of Minerals* **29**, 668–679.

Wang, R., Che, X., Zhang, W., Zhang, A., & Zhang, H. (2009) Geochemical evolution and late re-equilibration of Na-Cs-rich beryl from the Koktokay #3 pegmatite (Altai, NW China). *European Journal of Mineralogy* **21**, 795–809.

Wise, M.A. & Brown, C.D. (2010) Mineral chemistry, petrology and geochemistry of the Sebago granite-pegmatite system, southern Maine, USA. *Journal of Geosciences* **55**, 3–26.

Received April 16, 2014, revised manuscript accepted September 16, 2014.